NASA-CR-193025

THE ORIGIN AND EVOLUTION OF DUST IN INTERSTELLAR AND CIRCUMSTELLAR ENVIRONMENTS

GRANT
IN-90-CR
161915
P. 58

Status Report, April 1993

Principal Investigator: Douglas C. B. Whittet

Co-Investigator: Chun M. Leung

NASA Grant Number: NAGW-3144

Department of Physics,
Rensselaer Polytechnic Institute,
Troy, NY 12180.

(NASA-CR-193025) THE ORIGIN AND EVOLUTION OF DUST IN INTERSTELLAR AND CIRCUMSTELLAR ENVIRONMENTS Status Report, 1 Jul. 1992 - 30 Apr. 1993 (Rensselaer Polytechnic Inst.) 58 p

N93-27287

Unclas

G3/90 0161915

1. Introduction

This status report covers the period from the commencement of the research program on July 1, 1992 through April 30, 1993. Work is in progress on various topics described in the original proposal, and these are summarized below. Significant results have already been obtained: two papers arising from this work have been accepted for publication.

2. Grain Formation in Circumstellar Envelopes

We have begun a detailed study of the grain formation problem in stellar outflows. Grain formation consists of nucleation followed by growth. Most studies have used classical nucleation theory to describe the formation rate of grain nuclei in a supersaturated vapor, under the assumption of local thermodynamic equilibrium. The nucleation process, however, is best determined by solving a system of kinetic equations. The growth of the nuclei is then determined by solving a set of moment equations which are highly dependent on the nucleation rate of particles in the gas. To test the validity of classical nucleation theory in astrophysical environments, a truncated set of kinetic equations is solved simultaneously with the moment equations, thus allowing a self-consistent treatment of grain nucleation and growth. It is found that classical nucleation theory allows nucleation of grains to occur at a much lower supersaturation than is calculated from the kinetic equations, thus predicting dust formation too close to a star, overestimating the number of dust grains produced, and underestimating the average grain size. The effects of these results on the dynamics of outflow and radiative transfer in the dust shell are being investigated, in particular, the effects of grain formation on the dynamics of stellar outflows and vice versa.

3. Photochemistry in Circumstellar Envelopes

Evolved stars and their circumstellar envelopes (CSEs) play an important role in replenishing the interstellar medium (ISM) with dust and various molecular and atomic species. CSEs are also rich chemical environments with many different molecular species observed. In previous studies of photochemistry in CSEs, many authors applied semi-analytic approximation to treat the transfer of the continuum radiation, ignored scattering by dust, or used a small set of chemical reactions. To understand the coupling between the radiation field and the chemistry, we have constructed a comprehensive model including detailed ion-molecule chemistry, self-shielding of CO and H_2, and solve self-consistently for the continuum radiation field. We have concentrated on studying the photodissociation of CO and the relatively fast ion-molecule chemistry that ensues. We find that the errors introduced by the analytic approximation for the continuum transfer are appreciable: for example, the CO abundance differs by two orders of magnitude between the analytic and self-consistent solutions. We also find that the difference in CO and C^+ abundance have a pronounced effect on the chemical abundance of more complicated species, especially hydrocarbons. We conclude that detailed reaction networks and the self-consistent determination of the radiation field are necessary to accurately model the ion-molecule chemistry in evolved CSEs. Our next step is to incorporate grain-surface chemistry and hydrodynamics into these models.

4. Modeling Ice Features in Circumstellar Envelopes

In the cool, thick circumstellar envelopes of O-rich evolved stars, water molecules condense onto previously formed silicate grains to form ice mantles which exhibit an infrared absorption feature at 3.1 μm. The absorption coefficients for molecular ices change with temperature mostly due to an irreversible phase change in the ice from an amorphous state to a crystalline state at around 100 K. This effect narrows the feature and increases the peak strength as the temperature increases. Using laboratory measured optical constants we have constructed radiation transport models to determine what changes this effect would have on the observed 3 μm feature. We find that the

amorphous ice feature is symmetric and shallower than the crystalline ice feature. Furthermore, for both types of ices, there is a big discrepancy between the actual optical depth used in the model and that derived by comparing the continuum flux with the observed flux at the peak of the feature. The discrepancy arises from the radiation emitted by the hot silicate grains in the inner region of the dust shell. If this emission is not taken into account, the derived optical depths and the dust densities can be off by up to a factor of five. The decrease in strength of the feature leads to a perceived broadening which could lead to a misidentification of the feature.

5. Episodic Dust Formation in Circumstellar Envelopes

A number of evolved stars show evidence for episodic dust formation. A characteristic of these objects is the presence of cool dust indicated by strong excess flux in the IRAS 60 μm band. We made a detailed infrared study of the prototype object HR 3126, a bright star embedded in a compact, self-generated reflection nebula associated with a bipolar outflow. Both the composition of the dust shell and the mechanism responsible for its ejection had previously been controversial. Our study (Chiar *et al.* 1993) presents new photometric and spectroscopic observations. The spectral energy distribution indicates that the shell contains dust with temperature in the range 35–1300 K. On the basis of near and mid-infrared spectroscopy, combined with an assessment of various color-color diagrams, we reject the hypothesis that HR 3126 is carbon-rich. A weak silicate emission feature is detected at 10 μm, and a previous report of silicon carbide emission at 11.2 μm is not substantiated. Our results are discussed with a view to discrimination between proposed scenarios for the evolutionary status of the star. We conclude that HR 3126 is in a phase of advanced and rapid post-main-sequence evolution, possibly beginning its ascent of the asymptotic giant branch. Studies of other members of this class of object are underway.

6. Grain Evolution in the Diffuse Interstellar Medium

The spectral dependence of interstellar extinction places useful constraints on the properties of diffuse interstellar dust. Previous work has shown that there is apparent convergence to invariant behavior in the extinction curve at infrared wavelengths. In order to test this apparent invariance in extreme environments, we carried out an investigation of the B-type star HD 62542 in the Gum Nebula (Whittet *et al.* 1993), an object previously known to have an exceptionally anomalous extinction curve in the ultraviolet. Our study shows that, in contrast, the infrared extinction law is normal, indicating a degree of independence between the properties of the larger grains producing optical and IR extinction and the smaller grains producing UV extinction. The properties of the larger grains are characteristic of amorphous semiconductors, in which the low energy absorptions are dominated by impurities which produce energy levels between valance and conduction bands.

7. Grain Evolution in Dense Molecular Clouds

We have continued development of an observing program for the Infrared Space Observatory, in parallel with a program of related ground-based observations. Whittet was awarded time on the UK Infrared Telescope in Hawaii (2 nights, July 1992), in collaboration with Chiar (RPI grad student), Adamson and Kerr (Lancashire Polytechnic), for investigations of the solid CO and water-ice features in the Serpens dark cloud. These observations were successfully completed and are currently being prepared for publication. Comparisons of this cloud with others previously investigated by our group are providing important insight into the relation between the physical properties and composition of interstellar ices and local environment. The relative abundances of CO and H_2O-dominated ices are a function of cloud age and evolutionary state.

8. Publications

Chiar, J.E., Whittet, D.C.B., Aitken, D.K., Roche, P.F., Smith, C., Walker, H.J., Whitelock, P.A. & Wright, C., 1993, *An infrared study of the remarkable dusty M star HR 3126*, ApJ, in press.

Whittet, D.C.B., Martin, P.G., Fitzpatrick, E.L. & Massa, D., 1993, *Interstellar extinction in the infrared: the molecular cloud towards HD 62542*, ApJ, in press.

To appear in
Ap. J. May 10, 1993

INTERSTELLAR EXTINCTION IN THE INFRARED: THE MOLECULAR CLOUD TOWARDS HD 62542

D. C. B. Whittet[1] [2], P. G. Martin[3],

E. L. Fitzpatrick[4] and D. Massa[5]

Received July 27, 1992; *accepted* November 2, 1992.

[1]Visiting astronomer, Cerro Tololo Inter-American Observatory, National Optical Astronomy Observatories, which are operated by the Association of Universities for Research in Astronomy, under contract with the National Science Foundation

[2]Department of Physics, Rensselaer Polytechnic Institute, Troy, New York 12180

[3]Canadian Institute for Theoretical Astrophysics, University of Toronto, Toronto, Ontario M5S 1A1

[4]Princeton University Observatory, Peyton Hall, Princeton, New Jersey 08544

[5]Applied Research Corporation, 8201 Corporate Drive, Landover, Maryland 20785

ABSTRACT

The B–type main–sequence star HD 62542 presents a rare opportunity to study the properties of interstellar grains in an unusual environment which may represent the interface between a dense cloud and an intercloud medium permeated by strong stellar winds and an intense ultraviolet radiation field. Anomalous extinction at ultraviolet wavelengths in this line of sight has been reported previously. We present near infrared photometry for the star and use it to investigate the interstellar extinction curve in the wavelength range 0.44–3.5μm. In common with previous studies of both diffuse and dense environments, we find that the extinction curve in the near infrared (1–4μm) is represented to a close approximation by the power law $A_\lambda \propto \lambda^{-1.8}$. We deduce the ratio of total to selective extinction to be $R_V = 3.24 \pm 0.05$, closely similar to the average value for diffuse clouds. From the resulting visual extinction ($A_V = 1.20 \pm 0.08$) and an assessment of the literature on the spectral type and luminosity of the star, we derive a distance of 405 ± 35 pc, which probably places the star within the Gum Nebula, although it appears to be behind the complex of dark and bright nebulosity in the line of sight. The normality of the extinction law in the visible and near infrared is in marked contrast to the anomalous ultraviolet extinction. The grains responsible for the ultraviolet extinction bump, the far ultraviolet extinction rise, and the blue–visual extinction (of which the latter determine R_V) clearly respond to environmental influences in different ways. Our results give tentative support to the view that the complex formed as an accumulation of diffuse–cloud material swept up by stellar winds and radiation, although a model based on ablation of a dense globule is not excluded.

Subject headings: ISM: dust, extinction — stars: individual (HD 62542)

1 Introduction

Interstellar matter in the line of sight to the B3–5 V star HD 62542 is remarkable in several respects. The region has an unusual morphology (see, e.g., figure 3 [plate 27] of Cardelli et al. 1990), bearing some resemblance to a cometary globule: it contains a roughly V–shaped complex of dark and bright nebulosity, $\sim 1^\circ$ in angular extent, with HD 62542 located approximately 10 arcmin North–West of the region of greatest optical opacity. The ultraviolet extinction curve of HD 62542 is highly anomalous (Cardelli & Savage 1988), displaying a weak mid-ultraviolet bump centered at significantly shorter wavelength (2110 Å) than the average value (2175 Å), and a steep far ultraviolet rise. The optical spectrum of HD 62542 exhibits CH and CN lines which imply exceptionally high molecular column densities for a line of sight with only ~ 1 magnitude of visual extinction (Cardelli et al. 1990). It seems clear that these properties are inextricably linked with physical conditions in the local environment, dominated by the proximity of two luminous early-type stars, ζ Pup and γ^2 Vel. Two scenarios appear capable of explaining the morphology and density of the region. The complex could represent a concentration of diffuse interstellar material swept up by the ambient stellar winds and radiation fields, with HD 62542 lying near the intersection of expanding bubbles centered on ζ Pup and γ^2 Vel in the Gum Nebula (Cardelli & Savage 1988). An alternative is that the region contains the remnant core of a dense molecular cloud that has lost its outer envelope due to stripping by winds and ultraviolet radiation (Cardelli et al. 1990). There are, indeed, a number of cometary globules in the Gum Nebula which are likely to have formed in this way (Reipurth 1983).

The HD 62542 complex undoubtedly has much to tell us about the evolution of dust in extreme environments and the relation between the various grain populations responsible for extinction at different wavelengths. In view of this, it is clearly important to investigate the extinction curve of HD 62542 over a wide spectral range in order to constrain the properties of the dust in the region. By combining ultraviolet and infrared data for stars with degrees of reddening roughly comparable to that of HD 62542, Cardelli et al. (1989) concluded that the extinction curve generally displays correlated changes from star to star in different wavelength regimes, variations which may be characterized by a single parameter,

the ratio of total to selective extinction ($R_V = A_V/E_{B-V}$). Martin & Whittet (1990) analysed infrared data for sources with a wider range of A_V, sampling both low and high density environments, and showed that the extinction curve converges to a common or 'universal' form for $\lambda > 1\mu$m, well-represented mathematically by a power law. However, the infrared photometry required to extend these studies to the line of sight to HD 62542 was previously lacking. In this paper, we report new broadband photometry in the J, H, K and L passbands. We determine the most probable spectral dependence of the near–infrared extinction law towards HD 62542, and use it to evaluate R_V, leading to an improved estimate of the distance to the star. Our extinction data are discussed in the context of a possible correlation with anomalous behavior in the ultraviolet, and we assess the impact of our results on the nature and origin of the interstellar complex in the line of sight to HD 62542.

2 Infrared Photometry

HD 62542 was observed with the 1.5 m telescope at the Cerro Tololo Inter–American Observatory (CTIO), Chile, on three successive nights, April 9–11, 1989. Sky conditions were excellent on each night. The instrument used was the CTIO single-channel InSb near infrared photometer. Data were obtained through a 5 mm (23 arcsec) aperture and standard J (1.25μm), H (1.65μm), K (2.20μm) and L (3.45μm) broadband filters. Sky subtraction was achieved using a 30–arcsec East–West chop and standard beam–switching techniques. Results were reduced to the CTIO photometric system described by Elias et al. (1982). Comparing results for the three nights, the magnitudes are consistent to within formal statistical errors, and only the average value for each filter is given here:

$$J = 7.633 \pm 0.020; \quad H = 7.591 \pm 0.011;$$

$$K = 7.568 \pm 0.016; \quad L = 7.52 \pm 0.05.$$

No infrared data for HD 62542 are currently available at wavelengths longer than 3.5μm. We note that it was not detected by the Infrared Astronomical Satellite (IRAS): there are

no sources listed in the IRAS Point Source Catalog within 2 arcmin of the position of the star. This implies an upper limit on its flux density at 12μm of ~ 0.25 Jy.

3 The Extinction Curve

3.1 Derivation and Modeling

The method of obtaining the extinction curve from broadband photometry involves the deduction of color excesses

$$E_{\lambda-V} = (\lambda - V) - (\lambda - V)_0 \tag{1}$$

from observed and intrinsic color indices, where subscript '0' denotes the intrinsic value and λ represents the appropriate passband. The color excesses are then divided by E_{B-V} to give standard normalization, and results plotted against λ^{-1}. This procedure assumes the star to have a normal photosphere, devoid of abundance anomalies or shell characteristics which could lead to non–standard intrinsic colors. B, V magnitudes and spectral classification are required in addition to the infrared data from §2: following Cardelli & Savage (1988), we adopt $V = 8.04$, $B - V = 0.17$ (from Cousins & Stoy 1962). A spectral type of B3 V is given in the Michigan Atlas (Houk 1978), and Strömgren photometry presented by Kilkenny (1978) indicates B3.5$\pm$0.5 from the locus of the star in the c_1, $(b-y)$ diagram if the standard reddening vector is used to deredden it onto the main sequence. Cardelli & Savage (1988) adopted type B5 V (Feast et al. 1955; Cousins et al. 1961; Cousins & Stoy 1962) for their derivation of the ultraviolet extinction curve, but noted that the IUE spectrum is consistent with types in the range B3–B5. There are no reports of emission lines or other peculiarities in the optical spectrum of the star.

In Table 1, we present values of $E_{\lambda-V}$ and $E_{\lambda-V}/E_{B-V}$ separately for spectral types B3 V and B5 V, deduced from BV and $JHKL$ photometry using intrinsic colors from Johnson (1966). Values of $E_{\lambda-V}/E_{B-V}$ for the average diffuse interstellar medium (ISM; $R_V \simeq 3.05$) and the ρ Oph dark cloud ($R_V \simeq 4.3$) are also listed in Table 1 for comparison (Martin

& Whittet 1990 and references therein). It is immediately apparent that the extinction curve of HD 62542 is not anomalous at these wavelengths and is closer to the 'diffuse ISM law' than the 'ρ Oph law'. Infrared excess emission which can lead to spurious inflation of the R_V value in Be stars and dust–embedded stars (Whittet & van Breda 1978) is clearly absent in the near infrared colors of HD 62542, a conclusion also supported by the lack of an IRAS detection.

In order to provide a firm basis for extrapolation of the extinction curve (Figure 1) to $\lambda^{-1} = 0$, necessary for precise evaluation of R_V, we applied non–linear least–squares fits to the data, as described by Martin & Whittet (1990). This assumes that the extinction curve for $\lambda^{-1} < 1\,\mu\mathrm{m}^{-1}$ takes the functional form $A_\lambda/E_{B-V} = e\lambda^{-\alpha}$, and thus

$$\frac{E_{\lambda-V}}{E_{B-V}} = e\lambda^{-\alpha} - R_V, \tag{2}$$

consistent with observational data for both diffuse and dense interstellar clouds. The fits are illustrated in Figure 1, and the resulting values of the relevant parameters are listed in Table 2. Data for the diffuse ISM and ρ Oph (Martin & Whittet 1990) are again shown for comparison. It is notable that all derived values of the spectral index α are consistent with $\alpha = -1.8$. We also note that the fit for HD 62542 is better, and the formal errors in α, e and R_V are appreciably lower, for spectral type B3 V compared with B5 V. In view of this and the discussion above, we adopt a spectral type of B3 V, and thus deduce $E_{B-V} = 0.37 \pm 0.02$ and $R_V = 3.24 \pm 0.05$ as the most probable values of the reddening and the ratio of total to selective extinction, respectively. The total visual extinction is thus $A_V = R_V E_{B-V} = 1.20 \pm 0.08$.

3.2 The Dependence of R_V on Galactic Longitude

Although an average value of $R_V \simeq 3.1$ is often used globally to characterize the extinction law for low–density interstellar material, Whittet (1977) noted a small but significant variation in R_V with galactic longitude (ℓ) for stars within 10° of the galactic plane. This variation is described by the equation

$$R_V = R_0 + R_1 \sin(\ell + \theta) \tag{3}$$

where $R_0 = 3.08 \pm 0.03$, $R_1 = 0.17 \pm 0.06$, and $\theta = 175° \pm 20°$. The effect was attributed to systematic changes in the average grain size, and it appears to arise due to a directional variation in the contribution of dust associated with the local OB star system (Gould's Belt) to the total extinction in any given line of sight (Whittet 1979). HD 62542 is situated at galactic coordinates $\ell = 255.9°$, $b = -9.4°$. Substitution for ℓ in equation (3) leads to a value of $R_V = 3.24 \pm 0.09$, in excellent agreement with the value derived from the extinction curve in §3.1 above. Thus, the modest increase in R_V for HD 62542 compared with the average value for the diffuse ISM can be understood in terms of the angular proximity of the line of sight to the direction of the center of Gould's Belt (Whittet 1979). Thus, there is no evidence for any deviation in R_V attributable to physical conditions specific to the interstellar cloud in the line of sight to HD 62542.

3.3 Comparison with polarimetric data

Clayton et al. (1992) have reported observations of linear polarization due to aligned grains towards HD 62542, combining spectropolarimetry in the satellite ultraviolet with ground-based data at optical wavelengths. Both optical and ultraviolet data are consistent with a fit based on the well-known Serkowski–Wilking empirical formula commonly used to describe the spectral dependence of interstellar polarization at visible wavelengths (Serkowski et al. 1975; Wilking et al. 1980, 1982; Whittet et al. 1992). There is no evidence for excess polarization associated with the 2175 Å feature in this line of sight. The peak value of the polarization, and the wavelength at which this occurs, are $p_{\max} = 1.38\%$ and $\lambda_{\max} = 0.59\mu$m, respectively. The latter quantity is correlated with R_V (Serkowski et al. 1975) and shows similar systematic behavior with respect to galactic longitude (§3.2). On the basis of the correlation reported by Whittet & van Breda (1978), $R_V \simeq 5.6\lambda_{\max} \simeq 3.3$ for HD 62542, which is again consistent with the value obtained independently from the extinction curve (§3.1).

The alignment efficiency is represented by the ratio of the degree of polarization to reddening or extinction. We deduce $p_{\max}/E_{B-V} \simeq 3.7\%$ mag^{-1} for HD 62542, a result which is appreciably lower than typical values (e.g. Serkowski et al. 1975). This could be attributed to depolarization due to the presence of twisted magnetic field lines or multiple clouds with different field geometries in the line of sight, or it could simply imply an unfavorable viewing angle relative to the average direction of the magnetic field aligning the grains. The absence of detectable rotation of the position angle of polarization with wavelength (Clayton et al. 1992) tends to favor the latter explanation.

3.4 R_V and the 2175Å feature

Cardelli et al. (1989) discuss characterization of the entire extinction curve in terms of a single parameter, which they take to be the reciprocal of R_V. In that work, the strength of the 2175 Å ultraviolet extinction bump is defined as the excess extinction in the feature with respect to a linear continuum. Setting $x = \lambda^{-1}$, the form of the extinction curve in the range $3 < x < 6\,\mu\text{m}^{-1}$ may be described mathematically by the empirical relation

$$\frac{E_{\lambda-V}}{E_{B-V}} = c_1 + c_2 x + c_3 D(x) \tag{4}$$

where c_1, c_2 and c_3 are constants for a given line of sight, and

$$D(x) = \frac{x^2}{(x^2 - {x_0}^2)^2 + \gamma^2 x^2} \tag{5}$$

is the Drude function representing the profile of the bump (Fitzpatrick & Massa 1986). In equation (5), x_0 is the position of the bump ($x = x_0$ at peak absorption), and γ is its width (FWHM), both in units of μm^{-1}. The strength of the bump per unit E_{B-V} relative to the linear term $(c_1 + c_2 x)$ in equation (4) is then

$$\frac{A_{\text{bump}}}{E_{B-V}} = \frac{c_3}{\gamma^2}, \tag{6}$$

and substituting $E_{B-V} = A_V/R_V$, we have

$$\frac{A_{\rm bump}}{A_V} = \frac{c_3}{\gamma^2 R_V}. \qquad (7)$$

The grains which carry the bump and the grains responsible for blue–visual reddening are likely to be separate populations which are nevertheless well mixed in the ISM, and which may respond to different physical conditions in a correlated way (Cardelli et al. 1989; Cardelli & Clayton 1991; Mathis & Cardelli 1992). Cardelli et al. examined the empirical correlations of $A_{\rm bump}/A_V$ and $A_{\rm bump}/E_{B-V}$ with R_V^{-1}, and found that, whereas the former shows a significant degree of correlation, the latter shows little or none. These plots are illustrated in Figures 2 and 3, respectively, combining the data set used by Cardelli et al. (1989) with UV data for HD 62542 from Cardelli and Savage (1988) and R_V from §3.1 above. These plots do not provide convincing evidence for any physical relationship between the two populations. Note that the correlation in Figure 2 is implied by equation (7) if c_3 and γ are independent of R_V. Figure 3 shows that $A_{\rm bump}/E_{B-V}$ is constant to within a factor of ~ 3 independent of R_V: the presence of scatter reflects variations in the abundance and/or the physical properties of the bump absorber from one line of sight to another, and HD 62542 is seen to be an extreme case in which $A_{\rm bump}/A_V$ is a factor ~ 2 lower than expected.

4 The Environment

4.1 Distance and Location of HD 62542

The absolute visual magnitude (M_V) of HD 62452 may be estimated independently from the MK spectral type (B3 V; see §3.1) and from the observed Hβ index ($\beta = 2.690$; Kilkenny 1981). These give values of -1.3 and -1.1, respectively (Kilkenny 1981 and references therein), and we adopt the mean of these two results, i.e. $M_V = -1.2 \pm 0.1$. With $V = 8.04 \pm 0.01$ (Cousins & Stoy 1962; Kilkenny 1978) and $A_V = 1.2 \pm 0.08$ (§3.1), the standard photometric distance equation yields a distance of

$$d = 405 \pm 35 \text{ pc.} \quad (8)$$

This result is comparable with (but more precise than) previous estimates, i.e. $d \sim 400$ pc (Cardelli & Savage 1988) and 400–500 pc (Cardelli et al. 1990).

The location of the star with respect to interstellar matter in the line of sight is discussed in detail by Cardelli & Savage (1988) and Cardelli et al. (1990). These authors conclude that it lies either within or just behind the Gum Nebula. The Gum Nebula is a bubble–like structure of diameter ~ 250 pc, centered at a distance of ~ 400 pc in a direction some 10° from the line of sight to HD 62542 (see Cardelli & Savage 1988 for references). For spherical geometry, our distance estimate places the star within the confines of the nebula. Nevertheless, it seems likely that the star lies in a low density region *behind* rather than *within* the molecular cloud in the line of sight. Inspection of the SRC Schmidt Survey J film (field 311) gives no indication of the presence of optical emission or reflection nebulosity in the region which is *illuminated by HD 62542 itself.* The lack of infrared excess emission lends further weight to the conclusion that the star is not embedded in dense interstellar material but lies behind it by chance alignment.

4.2 Associated IRAS Sources

Although there is no IRAS point source coincident with the position of HD 62542 itself, Cardelli & Savage (1988) noted the presence of 16 sources within 20 arcmin of the star listed in the IRAS Point Source Catalog (IPSC), apparently associated with the interstellar complex in the line of sight. It is of interest to know whether star formation is being triggered in the region. In order to assess this possibility, we have extracted flux densities for a total of 22 sources, including 6 identified in the IRAS Serendipitous Survey Catalog (ISSC) in addition to those in the IPSC. Results are listed in Table 3, and a chart showing the location of the sources relative to HD 62542 and the interstellar complex appears in Figure 4. Only three (#5, #6 and #22) are detected at 12μm. Comparison of the SRC J and I films indicates the presence of a red star at the position of each of these three sources.

Sources #6 and #22 have flux density ratios $F(12)/F(25) > 2$, and are thus unlikely to be pre–main–sequence (PMS) objects: both are probably late–type field stars. Source #5 has $F(12) \sim F(25)$, consistent with a PMS star. Source #20 is detected at 25, 60 and 100μm, displaying a spectral energy distribution that rises steeply with increasing wavelength. The remaining sources in Table 3 are detected at 60 and/or 100μm only, and many of them carry "cirrus" or "extended" flags in the IPSC. It is possible that some of these sources may be obscured galaxies, but most probably arise due to emission from clumps of warm dust in the complex: they are generally coincident with regions of high optical opacity on the survey films. Source #20 appears to be associated with the densest of these clumps. With the possible exception of source #5, there is a lack of good candidate young stellar objects in the IRAS database, consistent with the absence of known T Tauri stars in this region of the Gum Nebula (Pettersson 1991). We conclude that there is no convincing evidence for current or recent star formation in the cloud towards HD 62542.

4.3 Dust Processing

We have shown (§3.1) that, in common with other regions, the dust towards HD 62542 displays a power–law extinction curve (equation 2) of index $\alpha \simeq -1.8$ in the near infrared, indicating a degree of stability in the composition and size distribution of the relatively large (radii $a \geq 0.1\mu$m) dust grains responsible for extinction at these wavelengths. Variations in R_V are attributed to changes in the relative extinction due to somewhat smaller grains which dominate the selective extinction in the blue and visual passbands (Martin & Whittet 1990 and references therein). Increased values of R_V are frequently observed in dense interstellar clouds (e.g. ρ Oph, Table 2), and these may reflect a reduction in the relative numbers of intermediate–size grains, due to selective destruction, coagulation, or some other form of processing. The rigorously normal value of R_V deduced for HD 62542 (§3) is thus much more surprising than the unexceptional form of the infrared extinction law. If we exclude the possibility that opposing growth and destruction mechanisms have somehow conspired to yield a normal size distribution, we are forced to conclude that the environmental factors which lead to increases in R_V in many dense clouds do not occur in the complex which

obscures HD 62542.

The unexceptional nature of the extinction law of HD 62542 in the infrared and blue–visible may be contrasted with the situation in the ultraviolet. Our findings are consistent with the results of Cardelli & Clayton (1991), who conclude that the bump and far UV extinction components produce little or no contribution at optical wavelengths and are modified by processes independent of those responsible for the R_V–dependent extinction law. Only two other stars, HD 29647 (Cardelli & Savage 1988) and VCT 10 (Cardelli & Clayton 1991), which both lie in dark clouds, are known to have bump features displaced to such short wavelength. Shifts in the position of a solid state feature can be caused by changes in mean particle size, and the stability of the central wavelength of the bump in many lines of sight, covering a range of R_V values, is usually taken to imply that the absorbers are in the small particle limit. Interestingly, as pointed out by Cardelli & Savage (1988), a feature centered at ~ 2110 Å is consistent with absorption by graphite *spheres* in the small particle limit, whereas a feature at 2175 Å places stringent constraints on particle shape (e.g. by specifying the axial ratio for spheroids) if this condition is to be satisfied (Draine 1989). Another interesting point is that the interstellar extinction curve bearing the closest resemblance to that for HD 62542, i.e., combining a weak or absent bump with a steep FUV rise, is that observed towards stars in the Small Magellanic Cloud (Prévot et al. 1984). The low metallicity of the SMC leads to a high number–density of carbon stars, and thus, presumably, to a high abundance of carbon–rich stardust entering its interstellar medium. It thus seems reasonable to attribute the FUV rise to carbon–rich small grains (but not graphite), a conclusion supported by the *circumstellar* extinction curve observed in the galactic C–rich object HR 4049 (Waters et al. 1989). If graphite is the carrier of the bump, it is most likely to be formed in the interstellar medium by radiative heating and annealing of amorphous carbon (Sorrell 1990, 1991). In the environment of the Gum Nebula, both radiative processing and shock processing are likely to occur, and the net effect might be to boost the number of very small carbon grains (e.g. PAHs) relative to those responsible for the bump. A potential problem with this scenario is that shock processing tends to destroy large silicate grains more readily than small carbon grains, according to Seab & Shull (1983), yet our study has shown that the large grain population is stable towards

HD 62542.

4.4 Implications for the Origin of the Complex

We noted in §1 that the complex towards HD 62542 may represent either a concentration of diffuse–cloud material or the remnant of a dense globule. In either case, the winds and radiation fields of nearby OB stars are implicated. On the face of it, our determination of a normal R_V value tends to favor the former explanation, but both scenarios require a somewhat surprising combination of circumstances. The diffuse cloud model requires that material is swept up until densities are sufficiently high that the abundances of CH and CN can be understood, and this must be achieved without significantly altering the size distribution of the grains responsible for the visual and infrared extinction whilst allowing sufficient processing of the smaller grains to explain the anomalous extinction in the ultraviolet. We note that differential acceleration due to radiation pressure may lead to spatial separation of the grains with respect to both size and composition. For a bimodal grain population, it is conceivable that this could lead to an excess of small absorbing grains over large dielectric grains in the complex, thus explaining the FUV extinction excess, but it is nevertheless surprising that the value of R_V is preserved.

Turning to the dense cloud model, it is useful to compare HD 62542 with HD 130079, a B9 V star with a similar degree of reddening ($E_{B-V} = 0.36$), obscured by a *quiescent* globule devoid of star formation activity. A recent study (Whittet & Chiar, in preparation) showed that $R_V \simeq 5.4$ for HD 130079, in stark contrast to the normal value for HD 62542. It is possible that if the HD 130079 cloud were subject to the environment of the HD 62542 cloud, it would evolve in a similar way, but this would require modification of the grain size distribution such that the R_V–value approached that in the ambient diffuse ISM. Ablation of mantles from core–mantle grains seems an attractive possibility, and the abundances of CH and CN might then be explained in terms of the ablation products; however, the presence of high R_V values in lines of sight where spectroscopic evidence for volatile mantles is lacking (e.g. Whittet & Blades 1980) suggests that coagulation (Jura 1980) is a more likely cause of high R_V in dense clouds; reversion to a 'normal' size distribution upon disruption of the

cloud then requires a reversal of coagulation.

5 Future Work

A number of future investigations may help to resolve some of the issues discussed in this paper. A few examples are given here. It would clearly be of interest to know if R_V remains the same in more opaque regions of the complex towards HD 62542: unfortunately, this may be difficult to determine due to a lack of other stars suitable for extinction curve determination. A more fruitful approach may be to measure the degree of linear polarization as a function of wavelength towards stars in the region, and thus to use λ_{max} to monitor spatial variations in grain size. This has the advantage that spectral type information is not required for the target stars, and it would simultaneously allow investigation of the magnetic field structure. Gas phase abundances should be derived for a greater range of molecular species, particularly those likely to be favored by grain surface reaction schemes. Finally, observations designed to detect the infrared emission features characteristic of polycyclic aromatic hydrocarbons in the nebulosity could prove rewarding and may help to establish the link between these molecules and the carriers of the ultraviolet extinction.

We are grateful to the referee, Jason Cardelli, for helpful comments. This research was supported in part by the National Science Foundation (grant AST–8800784), the NASA Long Term Space Astrophysics Program (grant LTSA–92–65), and the Natural Sciences and Engineering Research Council of Canada.

REFERENCES

Cardelli, J.A. & Savage, B.D., 1988, ApJ, 325, 864.

Cardelli, J.A. & Clayton, G.C., 1991, AJ, 101, 1021.

Cardelli, J.A., Clayton, G.C. & Mathis, J.S., 1989, ApJ, 345, 245.

Cardelli, J.A., Suntzeff, N.B., Edgar, R.J. & Savage, B.D., 1990, ApJ, 362, 551.

Clayton, G.C., et al., 1992, ApJ, 385, L53.

Cousins, A.W.J. & Stoy, R.H., 1962, Roy. Obs. Bull. no. 64.

Cousins, A.W.J., Eggen, O.J. & Stoy, R.H., 1961, Roy. Obs. Bull. no. 25.

Draine, B.T., 1989, in *IAU Symp. no. 135, Interstellar Dust*, eds. L.J. Allamandola & A.G.G.M. Tielens (Kluwer, Dordrecht), p. 313.

Elias, J.H., Frogel, J.A., Matthews, K. & Neugebauer, G., 1982, AJ, 87, 1029.

Feast, M.W., Thackeray, A.D. & Wesselink, A.J., 1955, MemRAS, 67, 51.

Fitzpatrick, E.L. & Massa, D., 1986, ApJ, 307, 286.

Fitzpatrick, E.L. & Massa, D., 1988, ApJ, 328, 734.

Houk, N., 1978, *Michigan Catalogue of Two-Dimensional Spectral Types for the HD Stars*, vol. 2, University of Michigan, Ann Arbor.

Johnson, H.L., 1966, ARevA&A, 4, 193.

Jura, M., 1980, ApJ, 235, 63.

Kilkenny, D., 1978, MNRAS 182, 629.

Kilkenny, D., 1981, MNRAS 194, 927.

Martin, P.G. & Whittet, D.C.B., 1990, ApJ, 357, 113.

Mathis, J.S. & Cardelli, J.A., 1992, ApJ, in press.

Pettersson, B., 1991, in *Low Mass Star Formation in Southern Molecular Clouds*, ed. B. Reipurth, ESO Scientific Report No. 11, p. 69.

Prévot, M.L., Lequeux, J., Maurice, E., Prévot, L. & Rocca–Volmerange, B., 1984, A&A, 132, 389.

Reipurth, B., 1983, A&A, 117, 183.

Savage, B.D., Massa, D., Meade, M. & Wesselius, P.R., 1985, ApJS, 59, 397.

Seab, C.G. & Shull, J.M., 1983, ApJ, 275, 652.

Serkowski, K., Mathewson, D.S. & Ford, V.L., 1975, ApJ, 196, 261.

Sorrell, W.H., 1990, MNRAS, 243, 570.

Sorrell, W.H., 1991, MNRAS, 248, 439.

Waters, L.B.F.M., Lamers, H.J.G.L.M., Snow, T.P., Mathlener, E., Trams, N.R., van Hoof, P.A.M., Waelkens, C., Seab, C.G. & Stanga, R., 1989, A&A, 211, 208.

Whittet, D.C.B., 1977, MNRAS, 180, 29.

Whittet, D.C.B., 1979, A&A, 72, 370.

Whittet, D.C.B. & Blades, J.C., 1980, MNRAS, 191, 309.

Whittet, D.C.B. & van Breda, I.G., 1978, A&A, 66, 57.

Whittet, D.C.B., Martin, P.G., Hough, J.H., Rouse, M.F., Bailey, J.A. & Axon, D.J., 1992, ApJ, 386, 562.

Wilking, B.A., Lebofsky, M.J., Martin, P.G., Rieke, G.H. & Kemp, J.C., 1980, ApJ, 235, 905.

Wilking, B.A., Lebofsky, M.J. & Reike, G.H., 1982, AJ, 87, 695.

Table 1: Color excesses and normalized extinction curves for HD 62542 (assuming spectral types B3 V and B5 V). Mean extinction curves for the diffuse ISM and the ρ Oph dark cloud (Martin & Whittet 1990) are also shown for comparison.

λ (Band) (μm)	$E_{\lambda-V}$ B3 V	$E_{\lambda-V}$ B5 V	$\frac{E_{\lambda-V}}{E_{B-V}}$ B3 V	$\frac{E_{\lambda-V}}{E_{B-V}}$ B5 V	$\frac{E_{\lambda-V}}{E_{B-V}}$ ISM	$\frac{E_{\lambda-V}}{E_{B-V}}$ ρ Oph
0.44 (B)	+0.37	+0.33	+1.00	+1.00	+1.00	+1.00
1.25 (J)	−0.86	−0.76	−2.32	−2.30	−2.25	−2.98
1.65 (H)	−1.00	−0.88	−2.70	−2.67	−2.58	−3.52
2.20 (K)	−1.08	−0.94	−2.92	−2.85	−2.77	−3.85
3.45 (L)	−1.15	−1.00	−3.11	−3.03	−2.93	−4.06

Table 2: Results of power law fits (equation 2) to data in Table 1.

Param.	B3 V	B5 V	ISM	ρ Oph
e	1.40 ± 0.03	1.29 ± 0.10	1.19 ± 0.01	1.90 ± 0.05
α	1.89 ± 0.19	2.08 ± 0.65	1.84 ± 0.03	1.85 ± 0.09
R_V	3.24 ± 0.05	3.11 ± 0.13	3.05 ± 0.01	4.26 ± 0.04

Table 3: IRAS identifications and flux densities for sources associated with the interstellar complex towards HD 62542†.

#	IRAS	RA	Dec	[12]	[25]	[60]	[100]
1	07392–4210S	13.3	05	0.11L	0.11L	1.54	1.4L
2	07392–4152	15.8	05	0.11L	0.11L	1.18	1.4L
3	07393–4159	20.0	44	0.25L	0.36L	0.69	3.56
4	07396–4210	41.5	45	0.11L	0.11L	2.04	20.9
5	07398–4150S	48.3	16	0.20	0.19	0.30L	1.4L
6	07399–4207	56.9	24	5.72	1.77	0.30L	1.4L
7	07402–4218	17.1	07	0.11L	0.11L	1.36	14.4:
8	07404–4212S	27.2	05	0.11L	0.11L	1.77	1.4L
9	07404–4159	29.6	07	0.25L	0.25L	1.33:	7.94
10	07406–4155	36.1	17	0.25L	0.25L	0.88	9.5L
11	07406–4219	40.1	20	0.25L	0.25L	2.01	30.1L
12	07407–4206	43.8	42	0.25L	0.25L	1.33	13.1:
13	07408–4207S	52.7	51	0.11L	0.11L	2.02	21.8
14	07409–4158S	56.8	53	0.11L	0.11L	0.30L	13.5
15	07410–4219	00.8	13	0.25L	0.25L	2.58	31.5L
16	07410–4209	01.8	40	0.25L	0.25L	1.35	20.8:
17	07411–4159S	06.9	04	0.13L	0.11L	1.22	1.4L
18	07412–4211	14.4	06	0.25L	0.25L	1.52	21.7:
19	07415–4213	30.6	10	0.26L	0.27L	1.57	27.3L
20	07416–4213	38.0	49	0.25L	0.14:	2.36	25.0:
21	07419–4216	59.2	50	0.52L	0.25L	4.60	49.6L
22	07420–4217	01.5	54	0.60	0.29L	3.66L	49.6L

† The columns are as follows: (1) a running number used for identification in the text and in Figure 4; (2) IRAS name (format HHMM.M, DDMM, followed by S for sources detected in the ISSC only); (3)–(4) remainder of the IRAS position (seconds of RA; arcseconds of Dec); (5)–(8) IRAS fluxes (Jy) without color correction in the 12, 25, 60 and 100μm bands, taken from the ISSC where available (sources 1, 2, 4, 5, 6, 7, 8, 13, 14 and 17), otherwise from the IPSC. L indicates an upper limit and : indicates an uncertain value.

FIG. 1

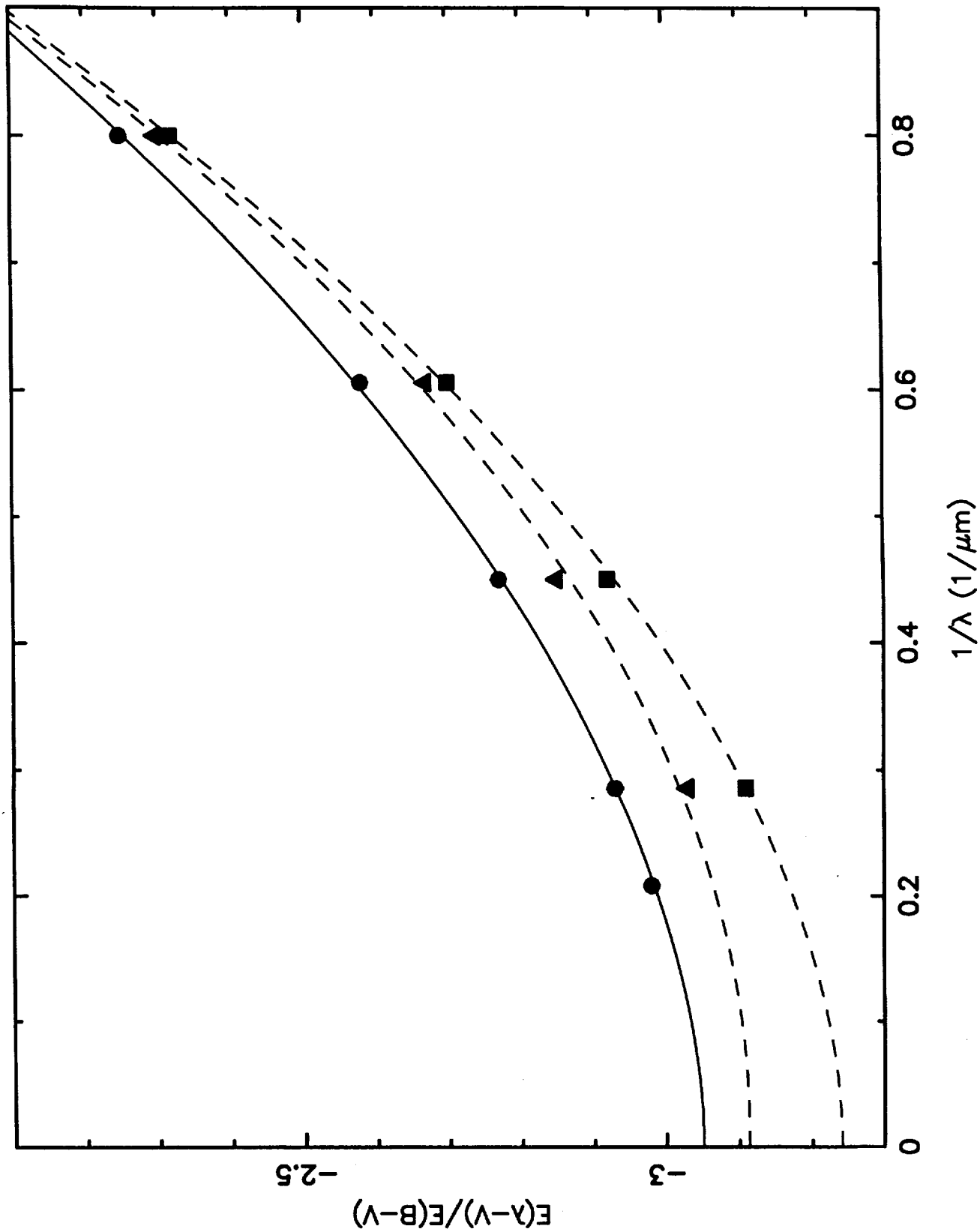

FIG. 2

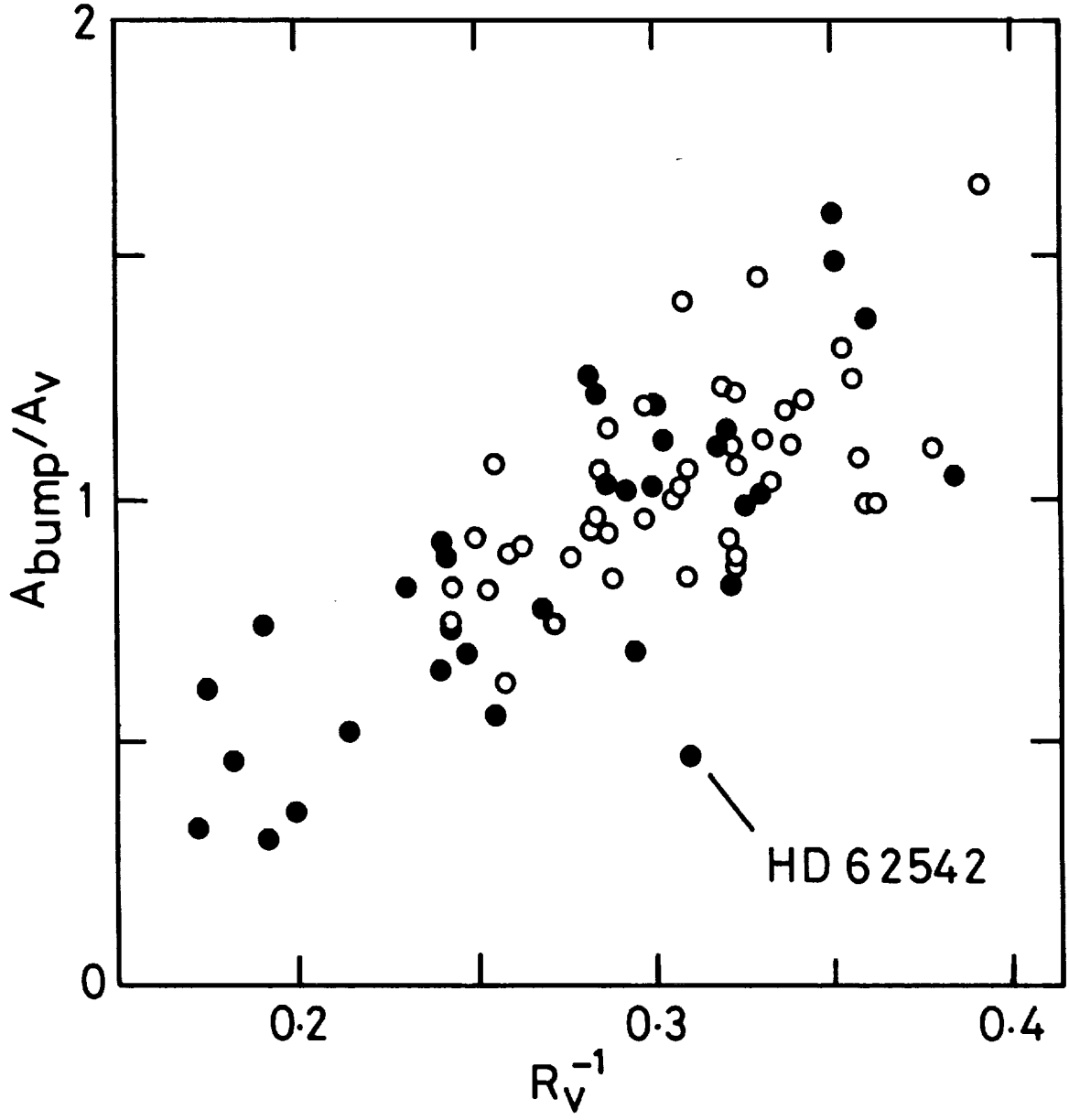

FIG. 3

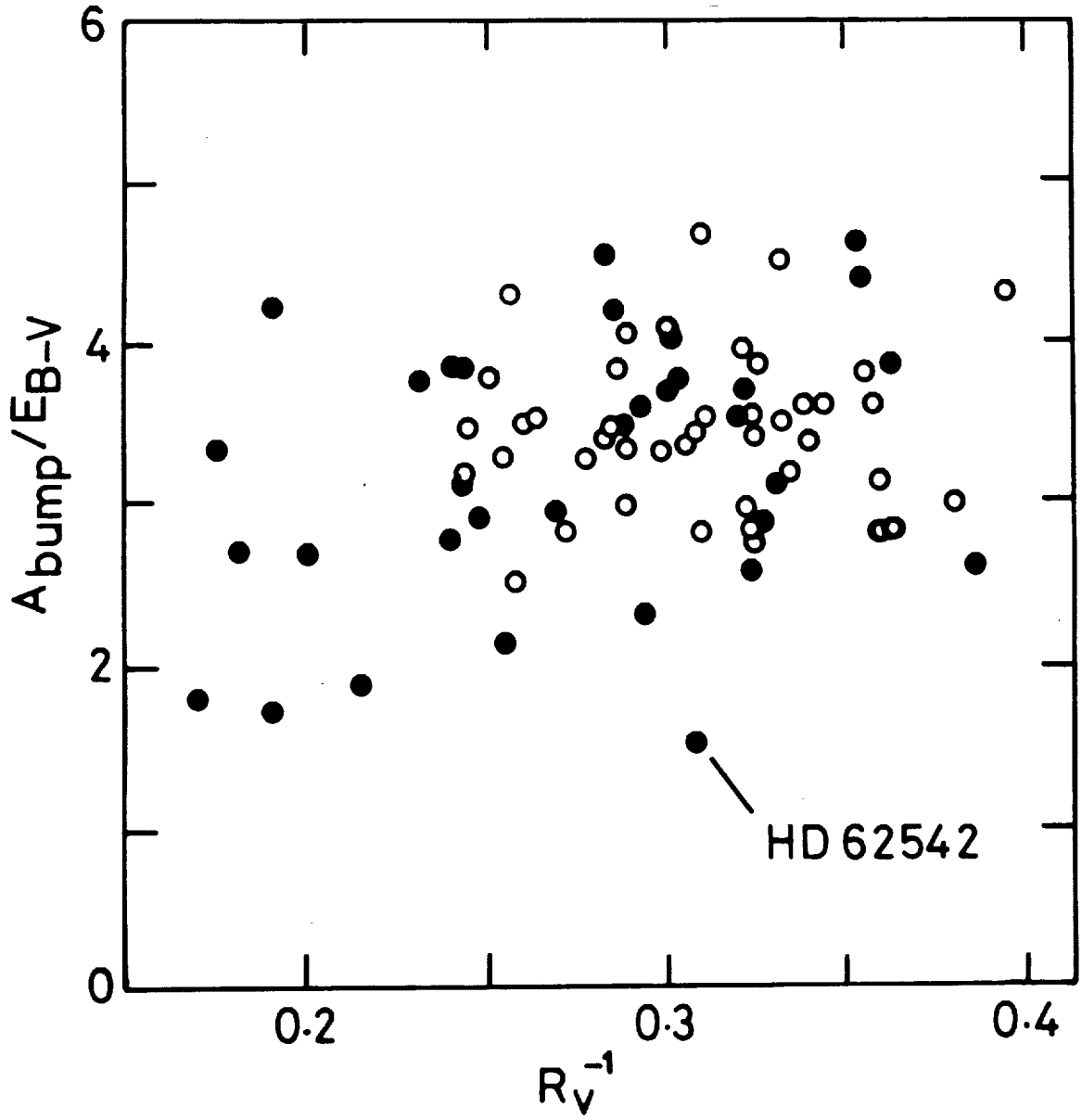

FIG. 4

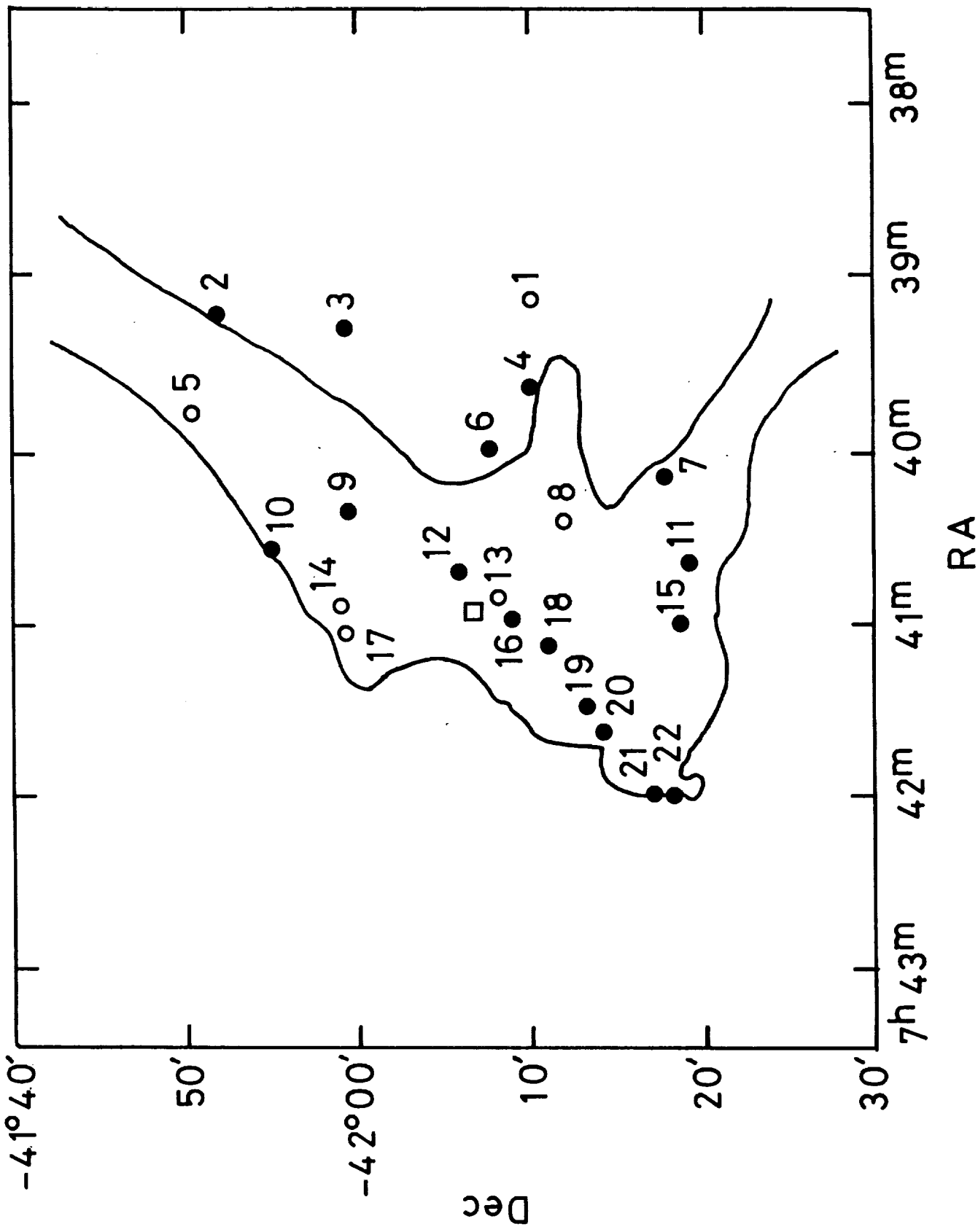
-41°40'
50'
-42°00'
10'
20'
30'
Dec
7h 43m
42m
41m
40m
39m
38m
RA
1
2
3
4
5
6
7
8
9
10
11
12
13
14
15
16
17
18
19
20
21
22

To appear in
Ap.J. May 20, 1993.

AN INFRARED STUDY OF THE REMARKABLE DUSTY M STAR HR 3126

J. E. Chiar [1], D. C. B. Whittet [1], D. K. Aitken [2],

P. F. Roche [3], C. H. Smith [2], H. J. Walker [4],

P. A. Whitelock [5] and C. Wright [2]

Received October 16, 1992; *accepted* November 10, 1992

[1]Department of Physics, Rensselaer Polytechnic Institute, Troy, New York 12180

[2]Department of Physics, Australian Defense Force Academy, University of New South Wales, Campbell, ACT 2600, Australia

[3]Department of Astrophysics, University of Oxford, Oxford OX1 3RH, UK

[4]Rutherford Appleton Laboratory, Chilton, Didcot, OX11 0QX, UK

[5]South African Astronomical Observatory, PO Box 9, Observatory, Cape 7935, South Africa

ABSTRACT

HR 3126 is a unique M giant star embedded in the bipolar reflection nebula IC 2220. Its evolutionary status is uncertain, and both the composition of the dust shell and the mechanism responsible for its ejection have proved controversial. In this paper, we present new photometric and spectroscopic observations of HR 3126, and combine them with existing data from the literature in an extensive reappraisal of its properties at infrared wavelengths. The spectral energy distribution is consistent with an optical classification of M0–3 II with infrared excess. The dust shell cannot be fitted by a single–temperature blackbody: at least three components are required, with temperatures in the range 35–1300 K. On the basis of spectroscopy at 1–4μm and 7–25μm, combined with an assessment of various color–color diagrams, we are able to reject the hypothesis that HR 3126 is carbon–rich. Weak silicate emission features are detected at 10 and 19μm, and a previous report of silicon carbide emission at 11.2μm is not substantiated. Our results are discussed with a view to discrimination between proposed scenarios for the evolutionary status of the star. Although it is not yet possible to draw definitive conclusions, it seems likely that HR 3126 is in a phase of advanced and rapid post–main–sequence evolution, possibly beginning its ascent of the asymptotic giant branch.

Subject headings: nebulae: reflection – photometry – stars: evolution, individual (HR 3126), mass loss, variables

1 Introduction

The association of a red giant with an optical reflection nebula is a rare event. To illustrate this point, consider the van den Bergh (1966) catalog of stars associated with reflection nebulae on Palomar Sky Survey prints: only 4 out of 187 stars listed are classified as M giants or supergiants[6]. In each of these cases, it seems likely from the morphology of the region that the star serendipitously illuminates ambient interstellar matter. Other examples of evolved stars embedded in nebulosity include the Cepheid RS Puppis (Westerlund 1961), the OH–IR star OH 231.8+4.2 (Cohen & Frogel 1977), the symbiotic proto–planetary nebula He 2–104 (Schwarz et al. 1989) and the bright M giant HR 3126 (Dachs & Isserstedt 1973). In each of these latter cases, there is strong circumstantial evidence to suggest that the visible nebula is the product of previous mass loss from the star (Havlen 1972; Allen et al. 1980; Schwarz et al. 1989; Perkins et al. 1981) rather than a random association. HR 3126 is unique in being the only known optically bright M giant to display a self–generated optical nebula.

In this paper, we examine the case of HR 3126 (HD 65750; V341 Car) and its circumstellar environment, with emphasis on observations at infrared wavelengths. We begin below with a brief overview of relevant literature. In subsequent sections, we investigate the photometric (§2) and spectroscopic (§4) properties of the star in the infrared, and model the broadband spectral energy distribution (§3). We also discuss (§5) constraints on the mass of the circumstellar nebula and attempt to reconcile them with the current mass loss rate of the star. The final section (§6) assesses the implications of our results: our goal is to discriminate between proposed scenarios for the evolutionary status of the star.

Optical spectra show HR 3126 to be a normal oxygen–rich M giant, classified variously as M3 III (Dachs & Isserstedt 1973), M1 II–III (Humphreys & Ney 1974), M1 II (Eggen 1974; Keenan & McNeil 1989), M0 III (Houk & Cowley 1975), and M2 II (Dachs et al. 1978). It

[6]The four M stars included in the van den Bergh catalog are HD 34454, HD 148478 (= α Sco), HD 187076 (= δ Sge) and BD+31° 4152; see Racine (1968) for more detailed spectral type information.

is therefore surprising to find discussion in the literature to the effect that HR 3126 may be carbon-rich (Thomas et al. 1976; Reimers 1977; Eggen & Iben 1991). The composition of the dust shell is constrained by solid state spectral features in the 8–20μm region. Thomas et al. (1976) find an 8–14μm excess peaking near 11.2μm, characteristic of SiC emission in carbon stars. However, Humphreys & Ney (1974) interpret data in the same spectral region in terms of 10 and 20μm emission features due to circumstellar silicate grains. Although silicate emission is, indeed, characteristic of some M giants, it is not usually seen in stars as early as M0–M3 in spectral type (Reimers 1977). There is evidence to suggest that the optical and near infrared colors of HR 3126 are also unusual for the spectral type: Eggen & Iben (1991) compare HR 3126 to three known carbon stars and show that there is little difference in the their spectral energy distributions between 0.4 and 3.4μm. The locus of HR 3126 in $(M_K, V-K)$ and $(M_{\rm bol}, R-I)$ diagrams is also that expected for a carbon star (see figure 6 of Eggen & Iben 1991). On the basis of these results and the strength of the emission in the IRAS passbands, Eggen & Iben are persuaded to think that HR 3126 is a thermally pulsating asymptotic giant branch (TPAGB) star that is dredging up carbon on its way to becoming a carbon star. Alternative evolutionary scenarios include an oxygen-rich star with core helium burning in the first red giant phase (Dachs et al. 1978), or a more evolved O-rich object which is ascending the asymptotic giant branch (Volk & Kwok 1987). Such proposals assume HR 3126 to be a single star, but the possibility exists that the star's evolution is being influenced by the presence of an unseen companion. We discuss these issues further in §6.

Optical photometry indicates that HR 3126 is an irregular variable with amplitudes of $\Delta V \sim 0.9^{\rm m}$ and $\Delta B \sim 1.1^{\rm m}$ (Dachs et al. 1978). Daily variations of $\Delta V \sim 0.10^{\rm m}$ have also been observed. No periodic brightness changes have been detected over a 15 year interval (Eggen 1974; Dachs et al. 1978; Eggen & Iben 1991), indicating an absence of pulsations. The photometric behavior of HR 3126 is thus somewhat similar to that of some M supergiants. On the basis of the $(B-V, V)$ color-magnitude diagram, Dachs et al. propose that variability is due to varying dust extinction in the surrounding nebula. The ratio of total to selective visual extinction ($R_V = A_V/E_{B-V}$) was estimated to be in the range $3 < R_V < 6$. For comparison, the average value of R_V for interstellar extinction towards M giants is 3.6 ± 0.3

(Lee 1970).

HR 3126 appears to be a former member of the cluster NGC 2516 (Dachs & Isserstedt 1973; Eggen 1974; Dachs et al. 1978), an important result as it provides information on the luminosity, mass and age of the star. HR 3126 is located $\sim 1.7°$ from NGC 2516, and its original membership is supported by a comparison of proper motion and radial velocity information. The distance of HR 3126 is poorly constrained by the range in absolute magnitude consistent with the MK spectral classification: luminosity classes II and III are reported by different authors, but class III is inconsistent with membership. However, Reimers (1977) estimates an absolute magnitude independent of MK type (using the Wilson–Bappu effect) which supports membership. If membership is accepted, then a rather precise distance of 375 ± 20 pc is implied for HR 3126 (Dachs 1970). The age and mass of the star are then constrained by the location of the turnoff point in the cluster H–R diagram to be $\sim 5 \times 10^7$ years and $\sim 5\,M_\odot$, respectively (Dachs et al. 1978).

The most remarkable feature of HR 3126 is undoubtedly the optical nebula IC 2220 (see Plate 5 of Whittet 1989 for a color illustration). This butterfly–shaped cloud has an angular diameter of 2.5 arcmin corresponding to a linear diameter of 0.27 ± 0.01 pc (Dachs et al. 1978). Perkins et al. (1981) have shown that the optical linear polarization of IC 2220 displays a centrosymmetric pattern typical of a reflection nebula illuminated by a central star. The degree of polarization is also within normal limits, suggesting that the dust grains in IC 2220 are not unusual. Witt & Rogers (1991) conclude from a comparison of the colors of the nebulosity and the illuminating star that the dust in IC 2220 has scattering properties characteristic of average interstellar dust. From a polarized intensity plot of the nebula, Perkins et al. show that it is bipolar and biconical in structure, displaying a very regular morphology which is symmetric about the N–S and E–W axes. Recent millimeter–wave observations of CO in IC 2220 (Nyman et al. 1992) demonstrate the presence of bipolar outflow from the star. The possibility that the nebula arises due to ambient interstellar matter in the vicinity of HR 3126 can therefore be discounted: it appears that HR 3126 is undergoing mass loss, thereby producing a circumstellar envelope containing dust which bears a strong resemblance to interstellar dust.

2 Photometric Properties

2.1 Near Infrared Photometry

Twelve sets of photometric measurements in the standard J (1.25μm), H (1.65μm), K (2.20μm) and L (3.45μm) passbands, covering the time interval 1975–1989, are presented in Table 1. The observations between JD 2442767 and JD 2443559 have previously been reported by Catchpole et al. (1979), to which the reader is referred for further technical details. The results listed here have been revised using the new standard magnitudes of Carter (1990) and thus differ slightly from the values given by Catchpole et al. The other measurements have not been published previously. Note that all observations were made at the Sutherland site of the South African Astronomical Observatory (SAAO) with the exception of those on JD 2447627.9, which were made at the Cerro Tololo Inter-American Observatory (CTIO). The latter measurements were originally reduced to the CIT photometric system (Elias et al. 1982), but the values presented here have been transformed to the SAAO (Carter) system (see Bessell & Brett 1988). The magnitudes in Table 1 thus form a coherent data set. Uncertainties in individual values are ± 0.02 ($JHKL$) for the CTIO data and ± 0.03 (JHK), ± 0.05 (L) for the SAAO data. Average magnitudes and standard deviations are listed at the foot of the Table 1.

It is clear from inspection of the data in Table 1 that HR 3126 displays only low-amplitude variability in the near infrared. Comparing our results with the optical photometry of Dachs et al. (1978) and Eggen & Iben (1991), it is evident that there is a trend of decreasing amplitude of variability with increasing wavelength. This is a common feature of pulsational variables. However, noting the absence of pulsations, Dachs et al. propose that variability is due to fluctuations in the degree of circumstellar extinction. This model predicts a correlation of color with magnitude, as previously found for $B - V$ and V, but no such trend is apparent in the $JHKL$ data: the brightest (JD 2443218) and faintest (JD 2442767) K magnitudes correspond to rather similar $J - H$, $H - K$ and $K - L$ colors.

Figure 1 compares the mean position of HR 3126 in the ($J - H$, $H - K$) diagram with a schematic representation of the distributions of various classes of late type star (adapted

from Bessell & Brett 1988). Two points are plotted for HR 3126, using the average values from Table 1 with and without correction for reddening. The mean reddening is assumed to be $E_{B-V} = 0.37$, based on the adopted M1 II intrinsic colors (§3). The corresponding values of E_{J-H} and E_{H-K} are 0.14 and 0.07, deduced from the reddening law used by Bessell & Brett. Note that these color excesses include both a circumstellar component and an interstellar component: if the interstellar component is the same as that towards the cluster NGC 2516, then it amounts to $E_{B-V} = 0.09$ (Dachs 1970). The uncorrected colors of HR 3126 correspond to a region of Figure 1 occupied by carbon stars, but dereddening places it in the domain of M supergiants. We note that the star *cannot* be dereddened onto the class III giant branch for any reasonable color excess and reddening law.

2.2 IRAS data

HR 3126 was detected as a bright point source (07559−5859) by the Infrared Astronomical Satellite (IRAS). The fluxes (without color correction) in the four IRAS passbands are 101.5, 43.9, 54.2 and 103 Jy at 12, 25, 60 and 100μm, respectively. Whereas the F_{12}/F_{25} ratio is within normal limits for a late–type star, HR 3126 clearly has a strong infrared excess at 60 and 100μm (see §3). The 60 and 100μm emissions are extended asymmetrically around the star on a scale ($\sim$ 20 arcmin) large compared with the extent of the visible nebula. This extended emission appears to be due to the presence of filamentary nebulosity ('cirrus') visible optically on the SERC Schmidt J films (fields 123 and 124) over much of the region and is unlikely to be physically associated with HR 3126 and IC 2220. In any case, examination of the 60 and 100μm contour plots (Waters, personal communication) indicates that the extended emission makes only a small contribution to the point source fluxes at these wavelengths.

The IRAS [12]−[25], [25]−[60] color–color diagram has been used as a diagnostic of the late stages of stellar evolution (e.g. van der Veen & Habing 1988, Walker et al. 1989). HR 3126 occupies an anomalous position in this diagram due to its unusually strong 60μm excess contrasted with a relatively normal [12]−[25] color, as illustrated in Figure 2, where HR 3126 is plotted along with other members of its LRS autoclass (see §4.2). This group contains

a total of 179 stars with closely similar 7–25μm spectral energy distributions (Cheeseman et al. 1989). The boxes in Figure 2 show the location of normal dust–free stars, together with optically identified O–rich and C–rich stars with thin dust shells (Walker & Cohen 1988), and demonstrating the unusual colors of HR 3126. HR 3126 has by far the most extreme [25] – [60] color of any member of this autoclass group.[7] A similar color anomaly occurs in the [25] – [60], [60] – [100] diagram. Van der Veen & Habing (1988) discuss the distribution of evolved stars in the [12] – [25], [25] – [60] diagram and propose a classification sequence. Its location places HR 3126 in class VIa, which is described thus: "...mainly non–variable stars with very cold dust at large distances. Some of them are carbon–rich; this is supported by the association of about 20% of the objects with cool carbon stars." Thus, the question of whether HR 3126 is O–rich or C–rich cannot be solved with reference to the IRAS broadband data alone.

Color–color diagrams which combine ground–based magnitudes with the IRAS [12] – [25] color appear to be particularly useful discriminators of C/O ratio in cool stars. One advantage of using such diagrams for HR 3126 is that they avoid a color based on the far infrared passbands where the infrared excess is strong. Epchtein et al. (1987) developed a classification scheme based on the $K - L$, [12] – [25] diagram: Fouque et al. (1992) use this system to classify HR 3126 as 'o2', a class consisting mainly of oxygen–rich stars. The [2.2] – [12], [12] – [25] diagram is also a good diagnostic (Hacking et al. 1985; Gaylard et al. 1989). A plot comparing the locus of HR 3126 with the distributions of various types of cool stars (Hacking et al. 1985) appears in Figure 3. The solid line shows the loci of blackbodies of various temperatures. Interestingly, HR 3126 lies in a region occupied by late M stars and is well separated from that occupied by carbon stars. This result clearly supports an O–rich composition for HR 3126.

Figure 3 also illustrates the fact that M stars with dust shells and M stars devoid of dust shells are well–separated in the [2.2] – [12], [12] – [25] diagram, and that this segregation is normally a function of spectral type. M0–M3 stars are usually devoid of dust, occupying

[7] It is interesting to note that HR 3126 has IRAS colors rather similar to those of Vega–like main–sequence stars with dust shells (Walker & Cohen 1988).

a region within the rectangular box close to the origin, whereas M4–M10 stars almost invariably have dust shells and are thus displaced upwards and to the right. As previously noted (§1), HR 3126 is anomalous in this respect: on the basis of its spectral type alone one would not expect it to have a dust shell.

3 Spectral Energy Distribution

Photometric data for HR 3126 covering the spectral range 0.34–100μm has been collected from the literature. As noted above (§1; §2.1), the star is optically variable with an amplitude that declines towards longer wavelength. Average magnitudes were calculated and converted to fluxes using standard calibrations (Wilson et al. 1972; Thomas et al. 1976; Bessell 1979). The resulting spectral energy distribution is plotted in Figure 4, in which the data sets of different authors are distinguished by plotting symbol. Mean results for each passband are listed in Table 2. The IRAS fluxes have been color corrected (*IRAS Explanatory Supplement, 1988*), assuming a blackbody temperature of 3000 K for HR 3126. Figure 5 plots mean ground–based data (0.3–5μm) together with IRAS broadband fluxes and low resolution spectrum.

In order to construct a model for the photospheric emission from the star, intrinsic colors for spectral types M0–M3 and luminosity classes I–III were extracted from the literature (Bessell & Brett 1988; Johnson 1966). Previous discussion (§1) suggests that HR 3126 is the most likely to be of luminosity class II: intrinsic colors for this class were estimated by averaging class I and class III colors. We found that spectral types in the range M0–M3 II give reasonable fits to the data for $0.34 < \lambda < 2.2\mu$m. Henceforth we adopt a type of M1 II, as illustrated in Figure 4. The intrinsic magnitudes were reddened using the standard average extinction law (Whittet 1992) and adjusted by an additive constant to correspond to the observed average magnitude at J (1.25μm). The values of reddening and visual extinction for this MK class are $E_{B-V} = 0.37$ and $A_V = 1.33$, the latter assuming $R_V = 3.6$ (see §1). Extrapolating the intrinsic color curve to 100μm, it is evident that HR 3126 has a large infrared excess at wavelengths $\lambda > 5\mu$m.

Models for the entire flux distribution of HR 3126 were constructed by combining the photospheric curve based on intrinsic colors for spectral type M1 II with blackbody curves representing the infrared excess due to circumstellar dust. Fits with a range of typical dust temperatures were attempted, and we found that a minimum of three blackbody curves is needed to give an adequate fit. A model using blackbody curves of temperatures 1300, 250 and 35 K is shown in Figure 5. Although not unique, this fit illustrates the wide range in grain temperature occurring in the envelope of the star. A previous estimate of 193 K for the color temperature of the dust continuum was obtained by Volk & Kwok (1987), who performed a least–squares fit of the Planck function to the four IRAS band fluxes. Whilst this result is within the range of temperatures implied by our investigation, we note that the infrared excess of HR 3126 cannot be adequately represented by a single–temperature blackbody.

Finally, we note that the spectral energy distribution clearly shows the presence of local excess emission peaking near 10μm, which we identify with silicates (see §4.2 below). This is evident in both the broadband data (Figure 4) and the LRS (Figure 5). In the latter case, the weaker 19μm silicate bending mode can also be discerned.

4 Infrared Spectroscopy

4.1 The 1–4μm Spectrum

A low–resolution near–infrared spectrum of HR 3126 covering the J, H, K and L windows was obtained with the 1.9m telescope at SAAO on December 28, 1981. The instrument used was the SAAO circular variable filter (CVF) spectrometer, which uses a nitrogen–cooled InSb detector and gives a mean spectral resolution of $\sim 0.02\mu$m. Standard beam–switching techniques were used. Cancellation of telluric absorption and flux calibration was achieved with reference to observations of Sirius. A brief description of the spectrum appears in Pesce et al. (1988). Figure 6 compares the spectrum of HR 3126 with that of HR 3950, a normal M2 III star observed in the same spectral region with the same telescope and instrument. The spectra are closely similar. Both show the expected dip at 2.3μm due to the unresolved

CO first overtone bandhead characteristic of M giants and supergiants (Merrill & Stein 1976; Arnaud et al. 1989), and its strength in HR 3126 is consistent with the adopted spectral type. There is a notable absence of broad H_2O absorption bands centered at 1.9 and 2.7μm (which partly overlap the telluric windows covered by these observations: see Merrill & Stein 1976); these bands are characteristic of Miras, and their absence in HR 3126 is consistent with the lack of long–period variability in the photometry. Significantly, the spectrum is also notably lacking in features characteristic of carbon stars, such as the C_2 bandhead at 1.77μm and the 2.9–3.2μm absorption feature due to unresolved HCN and C_2H_2 lines (Merrill & Stein 1976; Ridgway et al. 1978). The latter is a particularly sensitive indicator of the C/O ratio (Catchpole and Whitelock 1984) and its absence in HR 3126 indicates C/O$<$ 1 We conclude that the 1–4μm spectrum of HR 3126 is typical of a normal early M–type giant.

4.2 The Mid–Infrared Spectrum and the Silicate Feature

A low–resolution spectrum of HR 3126 covering the 7–13μm atmospheric window was obtained with the 3.9 m Anglo–Australian Telescope (AAT) at Siding Spring on May 18, 1992, using the University College London (UCL) spectrometer described by Aitken & Roche (1982). The observations were made with a beam size of 4.2 arcsec and a North–South chop of 20 arcsec. The spectral resolution was 0.23μm. Correction for telluric absorption and flux calibration was achieved with reference to observations of Canopus, taken as a 7000 K black body with a 10μm flux of 154 Jy.

The spectrum, presented in Figure 7, clearly confirms that HR 3126 has a silicate emission feature. A previous report (Thomas et al. 1976) of 11.2μm silicon carbide emission characteristic of C–rich circumstellar dust is not substantiated either by our AAT observations or by those made with the IRAS low resolution spectrometer (LRS; see Figure 5). Analysis of the latter data place HR 3126 (IRAS 07559−5859) in a weak silicate emission class (*Atlas of Low Resolution IRAS Spectra* 1986; Cheeseman et al. 1989), although the strength of the feature in the LRS seems somewhat lower than that implied by our ground–based observations (see below). Cheeseman et al. find that sources in this autoclass (25) are generally M

stars, and usually not very variable. The autoclass was further subdivided, and HR 3126 placed in a subclass with distinct (weak) 10μm and 19μm features, together with other known M stars. The suggestion of an SiC feature seems to arise largely from an apparent excess in a single intermediate passband centered at 11.2μm (Table 2; see also figure 5 of Thomas et al.). If this observation is disregarded, then all available mid–infrared data are consistent with the original conclusion of Humphreys & Ney (1974) that HR 3126 displays weak silicate emission. Silicate features in the spectra of carbon stars are not unknown (e.g. LeVan et al. 1992), but this possibility can almost certainly be rejected for HR 3126 on the basis other evidence.

We have attempted to model the silicate profile using techniques previously developed by Aitken & Roche (1982). Fits were obtained using emissivity functions derived from observations of the M supergiant μ Cephei, and the Trapezium cluster in the Orion nebula; in each case, the silicate emission is superposed on a multiple 1300 K and 3000 K blackbody continuum. The fits are illustrated in Figure 7 and both give acceptable agreement with the observations. (Somewhat surprisingly, the Trapezium emissivity function gives a marginally better fit: $\chi^2/N = 1.34$, compared with 2.52 for μ Cep.)

Volk & Kwok (1987) note a correlation between the strength of the silicate feature and the color temperature of the infrared excess in O–rich stars observed by the LRS (see their figure 4). This correlation appears to represent an evolutionary trend, with the silicate feature going into self–absorption as the dust shell becomes optically thick with the onset of rapid mass loss. Volk & Kwok define the strength of the silicate feature in terms of the index

$$s = 10 \ln\left\{\frac{F_{\rm cont}}{F_{\rm sil}}\right\}, \qquad (1)$$

where $F_{\rm sil}$ is the flux at the center of the feature at 9.7μm, and $F_{\rm cont}$ is the continuum flux at 9.7μm estimated by fitting the adjacent continuum. Volk & Kwok obtain a value of $s \simeq -1.8$ for HR 3126, indicating weak emission. Applying the same technique to the AAT spectrum, we obtain $s \simeq -4.2$, suggesting a somewhat stronger emission feature than is apparent from the LRS. The origin of this discrepancy is uncertain, but we note that

the two instruments must sample different environments since the AAT data were taken with a 4.2 arcsec aperture (and a 20 arcsec throw), whereas the LRS is an objective prism spectrograph with a 6 by 15 arcmin aperture mask so the spectrum of the star could be contaminated with emission from the surrounding nebula and from the known cirrus in the vicinity. In any case, the location of HR 3126 in the color–temperature *vs.* silicate index diagram is suggestive of the possibility that the star may be entering a phase of rapid mass loss.

5 On the Mass of the Circumstellar Envelope

The mass of the nebula surrounding HR 3126 is controversial. From the estimated circumstellar contribution to the observed reddening and the extent of the visible nebula in the plane of the sky, Dachs et al. (1978) estimate $M_{\rm neb} \sim 0.69\,{\rm M}_\odot$, a result based on the assumptions that (i) the gas-to-dust ratio in IC 2220 is the same as the average for the ISM, and (ii) the cloud is spherically symmetric. However, the observations of Perkins et al. (1981) imply the existence of a circumstellar *disk* which is seen almost edge–on, and the assumption of spherical symmetry thus leads to an overestimate of the mass. From the observed surface brightness, and assuming a grain size of 0.1μm, Perkins et al. estimate the nebular mass of IC 2220 to be $M_{\rm neb} \sim 0.01\,{\rm M}_\odot$ for graphite grains and $\sim 0.04\,{\rm M}_\odot$ for silicate grains. Nebular masses of this order cannot be supported by the current mass loss rate of the star, which Reimers (1977) estimates to be $\dot{M} \sim 4 \times 10^{-7}\,{\rm M}_\odot\,{\rm yr}^{-1}$. Assuming uniform expansion, the timescale to form the nebula is $t_{\rm exp} = r/v_{\rm exp} \sim 10^4$ years, where $v_{\rm exp} \simeq 13\,{\rm kms}^{-1}$ is the expansion velocity measured from the optical spectrum (Reimers 1977), and $r \sim 0.15\,{\rm pc}$ is the radius of the visible nebula (Witt & Rogers 1991). At the current rate, the total mass ejected in this time is $\sim 4 \times 10^{-3}\,{\rm M}_\odot$, a factor of 10 less than the nebular mass estimated by Perkins et al. (1981) for silicates.

We may easily show that the current luminosity of HR 3126 is capable of sustaining a much higher mass loss rate than that deduced by Reimers (1977). According to Reimers, $M_V = -2.9$, and hence $M_{\rm bol} = -4.4$. From Laing (1980), the luminosity in solar units is

related to $M_{\rm bol}$ by

$$\log L = 1.89 - 0.4 M_{\rm bol}, \tag{2}$$

and thus for HR 3126, we have $L = 4.5 \times 10^3\,{\rm L}_\odot$. If all energy released by the star were to be used in driving the outflow, then by conservation of momentum, $L/c = \dot{M} v_{\rm exp}$, and an upper limit on the mass loss rate of HR 3126 is thus given by

$$\dot{M}_{\rm max} = \frac{L}{c v_{\rm exp}} \sim 7 \times 10^{-6}\ {\rm M}_\odot\,{\rm yr}^{-1}. \tag{3}$$

This exceeds the measured value by a factor of nearly 20. If this rate were to apply over the expansion timescale, the ejected mass would be $\sim 0.08\,{\rm M}_\odot$, which is compatible with the nebular mass estimates of Perkins et al. (1981). It is therefore very probable that the mass loss rate was considerably higher in the recent past.

6 Discussion

HR 3126 is unique amongst optically bright evolved M stars, due to the presence of the apparently self–generated circumstellar envelope responsible for the bipolar optical nebula IC 2220 and the infrared excess emission. In this section, we attempt to eliminate some of the controversy surrounding this star and its circumstellar environment, and to provide some pointers for future research, with a view to gaining an understanding of its evolutionary status. The primary areas of debate are the C/O ratio, the surprisingly low mass loss rate, and the possibility of a binary companion.

The hypothesis that HR 3126 has already become carbon–rich lacks supporting evidence and can be rejected on the basis of both the spectroscopic and the photometric properties of the star. Our near infrared spectrum (§4.1) is consistent with the optical classification and conspicuously lacking in features characteristic of carbon stars. Our mid infrared spectrum (§4.2) does not support a previous report of SiC emission, but is in qualitative agreement with the LRS classification of HR 3126 as a weak silicate emitter. Color–color diagrams

combining ground–based and IRAS colors are shown to be good photometric discriminators which clearly separate HR 3126 from known carbon stars (§2.2). Thus, all available evidence supports the view that HR 3126 is, indeed, an oxygen–rich M–giant.

We noted in §1 that a number of contrasting evolutionary scenarios may be capable of explaining the observed properties of HR 3126. On the assumption that the presence of the nebula is in some way related to the current evolutionary status of the star, the suggestion of Dachs et al. (1978) that HR 3126 is in the *first* red giant stage can almost certainly be discounted: statistically we would expect to see many more nebulae associated with M giants if their ejection were a common characteristic of this evolutionary phase. A more likely possibility is that the star is ascending the asymptotic giant branch (AGB) and evolving towards a state where the circumstellar shell becomes optically thick and the silicate feature goes into self–absorption. This scenario is consistent with the O–rich classification and with the locus of the star in the IRAS color–temperature *vs.* silicate index diagram (Volk & Kwok 1987). The lack of other optically bright objects resembling HR 3126 may be explained in terms of the rapid onset of high circumstellar extinction which accompanies this phase, the star being seen at a time just before the point at which the shell becomes opaque at visible wavelengths. Although attractive, this model encounters an obvious difficulty in explaining the current mass loss rate (§5): Volk & Kwok (1987) suggest that $\dot{M} > 10^{-5}\,\mathrm{M}_{\odot}\,\mathrm{yr}^{-1}$ is needed to lead to silicate self–absorption, a limiting value which is comparable with our estimate of the *maximum* that can be supported by the star's current luminosity, and a factor ~ 25 higher than the empirical estimate. If this scenario is correct, then the low current mass loss rate must represent a temporary fluctuation. Recent studies of evolved stars with 60μm excesses detected by IRAS (Zijlstra et al. 1992) provide observational support for the view that mass loss on the AGB is not, indeed, a continuous process. Variations in mass loss rate may be interpreted theoretically in terms of luminosity changes associated with thermal pulses (Boothroyd & Sackmann 1988). Episodes of low mass loss may coincide with a decrease in or cessation of variability (Zijlstra et al. 1992), consistent with the observed properties of HR 3126.

Although we have shown that HR 3126 is not *currently* C–rich, the possibility remains that

it may be in a transitional phase between a normal O–rich red giant and a carbon star (Eggen & Iben 1991). Earlier phases of mass loss would lead to a dust shell composed predominantly of silicates, but dredge–up of carbon into the atmosphere to the extent that O and C have *comparable* abundances would lead to a dramatic decrease in the rate of dust nucleation; this would account for the weakness of the silicate feature, and would also provide a natural explanation of the low current mass loss rate if the outflow is driven primarily by radiation pressure on grains. The precursors of carbon stars are long–period variables with deep pulsations and high mass loss rates (Eggen & Iben 1991), but during dredge–up the pulsations die out, the mass loss rate declines, and the star becomes an irregular variable, consistent with the current light curve of HR 3126. According to Iben (1983), the transition may occur on a timescale as short as a few years.

Another possibility which requires investigation is that a number of the peculiarities of HR 3126 might be explicable in terms of the presence of a companion star, as originally suggested by Dachs & Isserstedt (1973). A possible prototype might be OH 231.8+4.2 (Cohen et al. 1985): this system contains an M9 III star, together with a blue companion which partly illuminates the surrounding biconical nebula, and Cohen et al. suggest that the companion may be implicated in the process which led to the ejection of the nebula. We note that the formation of planetary nebulae with bipolar morphologies appears to require close binary evolution (Livio 1992), and that the morphology of IC 2220 is similar to that of nebulae associated with symbiotic stars, which are also interpreted in terms of binary evolution. HR 3126 has infrared colors which are similar to those of both symbiotics and bulge M stars (Whitelock & Munari 1992). However, observational support for binarity in the case of HR 3126 is currently lacking. Radial velocity information is scanty, but two measurements separated by a decade (Eggen 1974; Andersen et al. 1985) are in close agreement. Dachs & Isserstedt (1973) invoked the presence of a blue companion to explain an apparent UV–excess in IC 2220, but Witt & Rogers (1991) conclude that the distribution of colors in the nebula may be explained entirely in terms of illumination by HR 3126 itself and the external interstellar radiation field.

In order to gain further insight into the evolutionary status of HR 3126, we recommend that

a high resolution study of the optical spectrum should be carried out. An important step would be a determination of abundances in the stellar atmosphere: a precise evaluation of the C/O ratio, for example, would help to distinguish between transitional AGB and transitional carbon–star scenarios. A re–evaluation of the expansion velocity and implied mass loss rate would also be timely. Finally, a time–resolved study of the radial velocity could provide evidence for the presence of a close binary companion of sufficient mass to influence the evolution of the star.

We are grateful to Chris Rogers and Rens Waters for providing us with CO and IRAS maps of the extended emission around HR 3126 in advance of publication, and for helpful discussion. We also thank Mike Fogel for providing us with his Planck curve fitting code. This research was partially supported by a grant from the NASA Long Term Space Astrophysics Program (LTSA–92–65).

REFERENCES

Aitken, D.K. & Roche, P.F., 1982, MNRAS, 200, 217.

Allen, D.A., Barton, J.R., Gillingham, P.R. & Phillips, B.A., 1980, MNRAS, 190, 531.

Andersen, J., et al., 1985, A&AS, 59, 15.

Arnaud, K.A., Gilmore, G. & Cameron, A.C., 1989, MNRAS, 237, 495.

Atlas of Low Resolution IRAS Spectra, 1986, IRAS Science Team, prepared by F.M. Olnon and E. Raimond, A&AS, 65, 607.

Bessell, M.S., 1979, PASP, 91, 589.

Bessell, M.S. & Brett, J.M., 1988, PASP, 100, 1134.

Boothroyd, A.I. & Sackmann, I.J., 1988, ApJ, 328, 632.

Carter, B.S., 1990, MNRAS, 242, 1.

Catchpole, R.M., Robertson, B.S.C., Lloyd Evans, T.H.H., Feast, M.W., Glass, I.S. & Carter, B.S., 1979, SAAO Circulars, 1, 61.

Catchpole, R.M. & Whitelock, P.A., 1984, in *Cool Stars with Excesses of Heavy Elements*, eds. M. Jaschek & P.C. Keenan, Reidel, p 19.

Cheeseman, P., Stutz, J., Self, M., Taylor, W., Goebel, J., Volk, K. & Walker, H., 1989, *Automatic Classification of Spectra from the Infrared Astronomical Satellite*, NASA Reference Publication 1217.

Cohen, J.G. & Frogel, J.A., 1977, ApJ, 211, 178.

Cohen, M., Dopita, M. A., Schwartz, R. D., & Tielens, A. G. G. M., 1985, ApJ, 297, 702.

Dachs, J., 1970, A&A, 5, 312.

Dachs, J. & Isserstedt, J., 1973, A&A, 23, 241.

Dachs, J., Isserstedt, J. & Rahe, J., 1978, A&A, 63, 353.

Eggen, O.J., 1974, PASP, 86, 960.

Eggen, O.J. & Iben, I., 1991, AJ, 101, 1377.

Elias, J.H., Frogel, J.A., Matthews, K. & Neugebauer, G., 1982, AJ, 87, 1029.

Epchtein, N., Le Bertre, T., Lepine, J.R.D., Marques dos Santos, P., Matsuura, O.T. & Picazzio E., 1987, A&A Supp, 71, 39.

Fouque, P., Le Berte, T., Epchtein, N., Guglielmo, F. & Kerschbaum, F., 1992 A&A Supp., 93, 151.

Gaylard, M.J., West, M.E., Whitelock, P.A. & Cohen, R.J., 1989, MNRAS, 236, 247.

Hacking, P., et al., 1985, PASP, 97, 616.

Havlen, R.J., 1972, A&A, 16, 252.

Houk, N., & Cowley, A.P., 1975, *Michigan Catalogue of Two-Dimensional Spectral Types for the HD Stars*, vol. 1, University of Michigan, Ann Arbor.

Humphreys, R.M. & Ney, E.P., 1974, A&A, 30, 159.

Iben, I., 1983, ApJ, 275, L65.

IRAS Catalogs and Atlases: Explanatory Supplement, 1988, eds. C.A. Beichman, G. Neugebauer, H.J. Habing, P.E. Clegg & T.J. Chester (Washington, DC).

Johnson, H.L., 1966, ARevA&A, 4, 193.

Keenan, P.C. & McNeil, R.C., 1989, ApJS, 71, 245.

Laing, K.R., 1980, *Astrophysical formulae*, 2nd edn., Springer–Verlag, Berlin, p. 563.

Lee, T. A., 1970, ApJ, 162, 217.

LeVan, P.D., Sloan, G.C., Little–Marenin, I.R. & Grasdalen, G.L., 1992, ApJ, 392, 702.

Livio, M., 1992, paper presented at IAU Symposium 155 *Planetary Nebulae.*

Merrill, K.M. & Stein, W.A., 1976, PASP, 88, 285.

Nyman, L.–A., Olofsson, H., Rogers, C., Heske, A. & Sahai, R., 1992, paper presented at ESO Conference *AGB stars.*

Pesce, J.E., Stencel, R.E., Walter, F.M., Doggett, J., Dachs, J., Whitelock, P.A., & Mundt, R., 1988, in *A Decade of UV Astronomy with the IUE Satellite*, ed. E.J. Rolfe, ESA Publication SP–281, 253.

Perkins, H.G., King, D.J. & Scarrott, S.M., 1981, MNRAS, 196, 403.

Racine, R., 1968, AJ, 73, 233.

Reimers, D., 1977, A&A, 54, 485.

Ridgway, S.T., Carbon, D.F. & Hall, D.N.B., 1978, ApJ, 225, 138.

Schwarz, H.E., Aspin, C., & Lutz, J.H., 1989, ApJ, 344, L29.

Thomas, J.A., Robinson, G. & Hyland, A.R., 1976, MNRAS, 174, 711.

van den Bergh, S., 1966, AJ, 71, 990.

van der Veen, W.E.C.J. & Habing, H.J., 1988, A&A, 194, 125.

Volk, K. & Kwok, S., 1987, ApJ, 315, 654.

Walker, H. J., & Cohen, M., 1988, AJ, 95, 1801.

Walker, H. J., Cohen, M., Volk, K., Wainscoat, R.J., Schwartz, D.E., 1989, AJ, 98, 2163.

Westerlund, B., 1961, PASP, 73, 72.

Whitelock, P.A., & Munari, U., 1992, A&A, 255, 171.

Whittet, D.C.B., 1989, in *IAU Symp. 135, Interstellar Dust*, eds. L.J. Allamandola & A.G.G.M. Tielens, p 455.

Whittet, D.C.B., 1992, *Dust in the Galactic Environment*, Institute of Physics Publishing, Bristol.

Wilson, W.J., Schwartz, P.R., Neugebauer, G., Harvey, P.M. & Becklin, E.E., 1972. ApJ, 177, 532.

Witt, A.N. & Rogers, C., 1991, PASP, 103, 415.

Zijlistra, A.A., Loup, C., Waters, L.B.F.M., & Jong, T., 1992, A&A, 265, L5 ~~in press~~.

Table 1: Infrared photometry of HR 3126

JD−2440000	J	H	K	L	Telescope†
2767.50	2.58	1.64	1.23	0.55	S30
2830.50	2.64	1.62	1.22	0.59	S30
3124.50	2.46	1.49	1.10	0.49	S30
3136.50	2.46	1.50	1.11	0.47	S30
3218.31	2.44	1.47	1.08	0.43	S30
3433.58	2.46	1.48	1.12	0.43	S30
3439.60	2.45	1.48	1.09	0.45	S30
3522.42	2.50	1.53	1.13	0.47	S30
3558.34	2.50	1.51	1.16	0.44	S30
5008.40	2.50	1.48	1.10	0.50	S40
7054.65	2.59	1.51	1.13	0.52	S30
7627.60	2.63	1.64	1.19	0.50	C60
Mean	2.518	1.529	1.138	0.487	
σ	0.070	0.062	0.048	0.047	

†Telescopes:
S30: SAAO 30–inch
S40: SAAO 40–inch
C60: CTIO 60–inch

Table 2: Mean fluxes from broad and intermediate passband photometry of HR 3126

λ (μm)	λF_λ (W m^{-2})	Reference†
0.34 (U)	6.86×10^{-13}	1, 2, 3
0.44 (B)	9.93×10^{-12}	1, 2, 3, 4
0.55 (V)	4.39×10^{-11}	1, 2, 3, 4
0.70 (R)	1.12×10^{-10}	3, 4
0.90 (I)	1.97×10^{-10}	3, 4
1.25 (J)	3.60×10^{-10}	4, 5
1.65 (H)	4.26×10^{-10}	4, 5, 6
2.2 (K)	2.86×10^{-10}	4, 5, 6
3.5 (L)	1.49×10^{-10}	4, 5, 6
4.8 (M)	6.44×10^{-11}	4, 6
8.5	2.78×10^{-11}	4, 6
9.7 (N)	2.37×10^{-11}	6
10.6	2.09×10^{-11}	4, 6
11.2	2.40×10^{-11}	6
12	1.79×10^{-11}	7
12.2	9.09×10^{-12}	4
12.5	1.21×10^{-11}	6
18	4.54×10^{-12}	4
25	3.79×10^{-12}	7
60	2.07×10^{-12}	7
100	2.83×10^{-12}	7

†References:

1. Bright Star Catalog
2. Dachs et al. (1978)
3. Eggen & Iben (1991)
4. Humphreys & Ney (1974)
5. This paper, Table 1
6. Thomas et al. (1976)
7. IRAS Point Source Catalog

FIGURE CAPTIONS

Figure 1: The $J - H$ versus $H - K$ diagram for late–type stars. The open circle with error bars shows the position of HR 3126 based on mean photometry from Table 1 without correction for reddening. Assuming a normal extinction law and $E_{B-V} = 0.37$ (see text), dereddening moves the locus of the star to the position of the filled circle with error bars. Also shown are areas occupied by carbon stars (dashed curve), oxygen–rich Miras and semiregular variables (dotted curve) and M–type supergiants (solid curve), and the giant sequence from G0 to M7 (solid line), adapted from Bessell & Brett (1988).

Figure 2: The [12] – [25] versus [25] – [60] diagram for the 179 members of IRAS LRS autoclass $\lambda 25$ (Cheeseman et al. 1989). Areas occupied by carbon stars and normal oxygen–rich stars are delineated by the upper and lower rectangles, respectively. HR 3126 is seen to have a much stronger 60μm excess than any other member of this class.

Figure 3: The [2.2] – [12] versus [12] – [25] diagram. The filled and open circles represent oxygen–rich stars of spectral type M0—M3 and M4—M10, respectively, and the crosses represent carbon stars (data from Hacking et al. 1985 for all stars except HR 3126). The rectangle at lower left shows the locus of normal stars without infrared excess. The line shows the locus of blackbodies as a function of temperature (K).

Figure 4: The spectral energy distribution of HR 3126, comparing observational data with the intrinsic color curve for spectral type M1 II. The symbols represent photometry from the following sources. Crosses: Bright Star Catalog; pentagons: Dachs et al. (1978); filled squares: Eggen & Iben (1991); open circles: Humphreys & Ney (1974); open squares: this paper, Table 1; stars: Thomas et al. (1976); filled circles: IRAS Point Source Catalog.

Figure 5: A fit to the spectral energy distribution of HR 3126. Triangles and filled circles represent mean ground–based fluxes and IRAS broadband fluxes, as listed in Table 2. The IRAS LRS spectrum is also shown. Dashed curves represent blackbodies of temperature 1300, 250 and 35 K. The model (continuous curve) combines the three blackbody curves with the M1 II intrinsic color curve shown in Figure 4.

Figure 6: The 1–4μm SAAO spectrum of HR 3126 (above) compared with that of the M2 III star HR 3950. The vertical axis is linear flux with arbitrary normalization.

Figure 7: The 7–14μm AAT spectrum of HR 3126. Two fits to the silicate feature are shown, using emissivity curves based on observations of μ Cephei (dotted curve), and the Trapezium (solid curve).

FIG. 1.

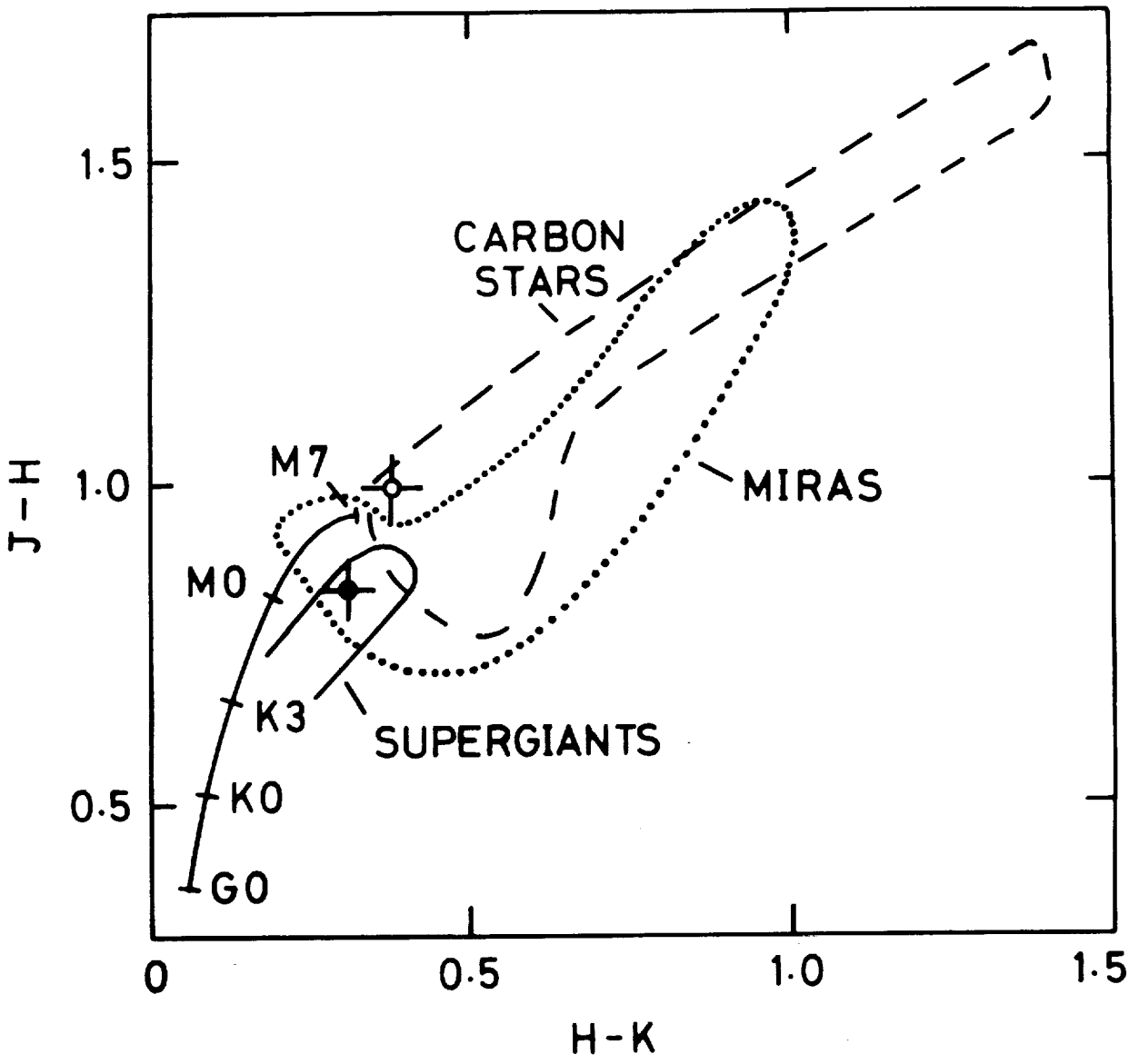
1.5
1.0
0.5
J-H
CARBON
STARS
M7
MIRAS
M0
K3
SUPERGIANTS
K0
G0
0
0.5
1.0
1.5
H-K

FIG. 2.

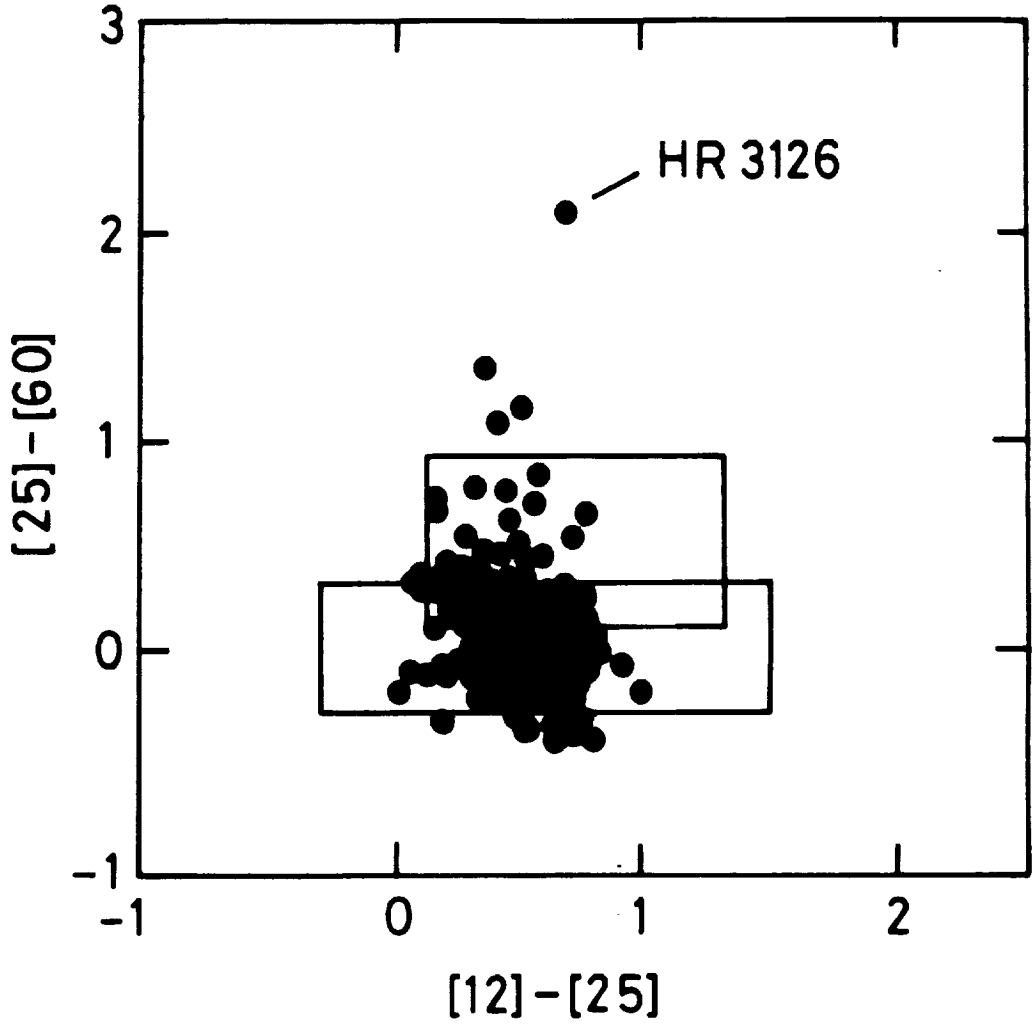

FIG. 3.

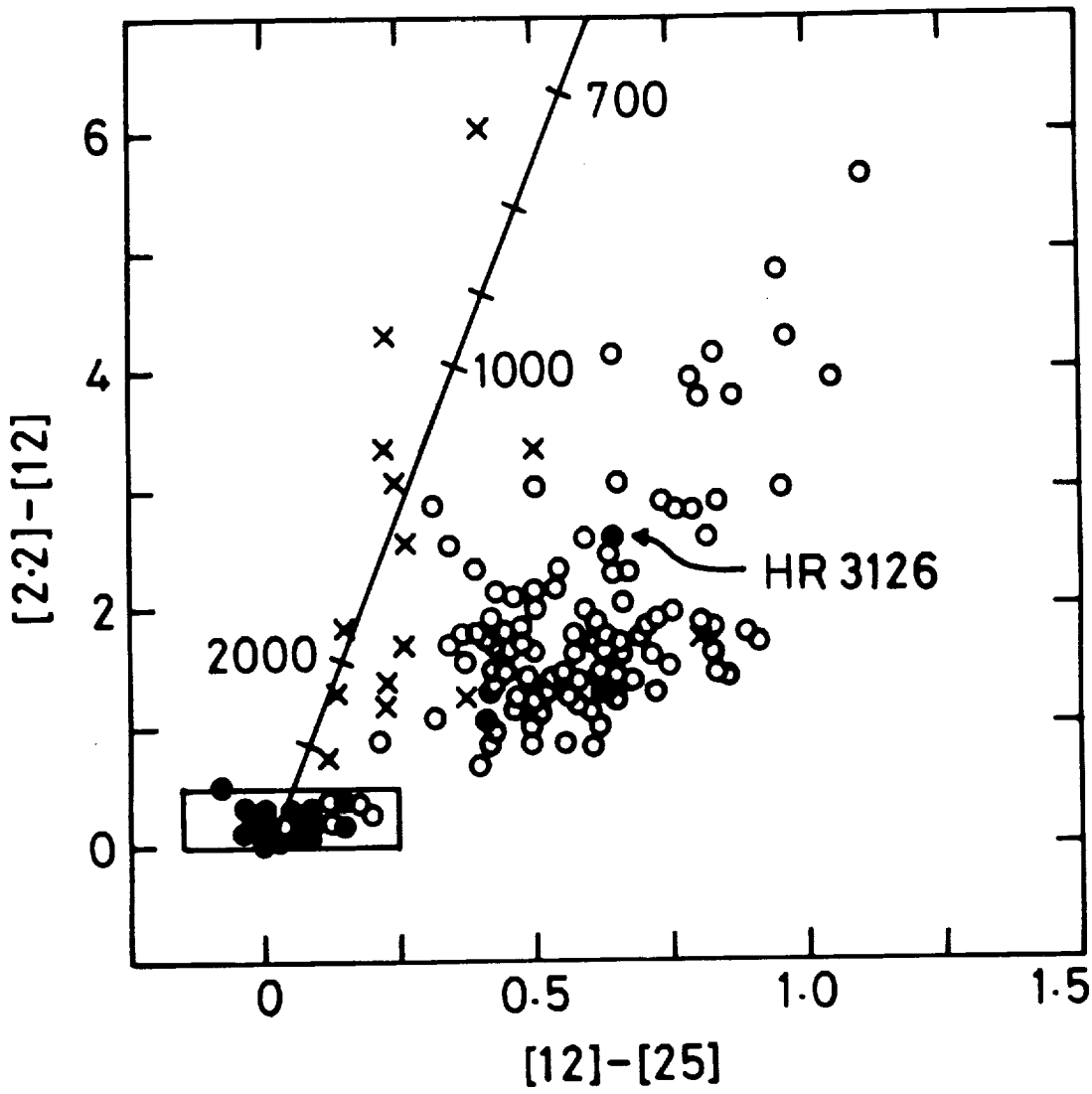

FIG. 4.

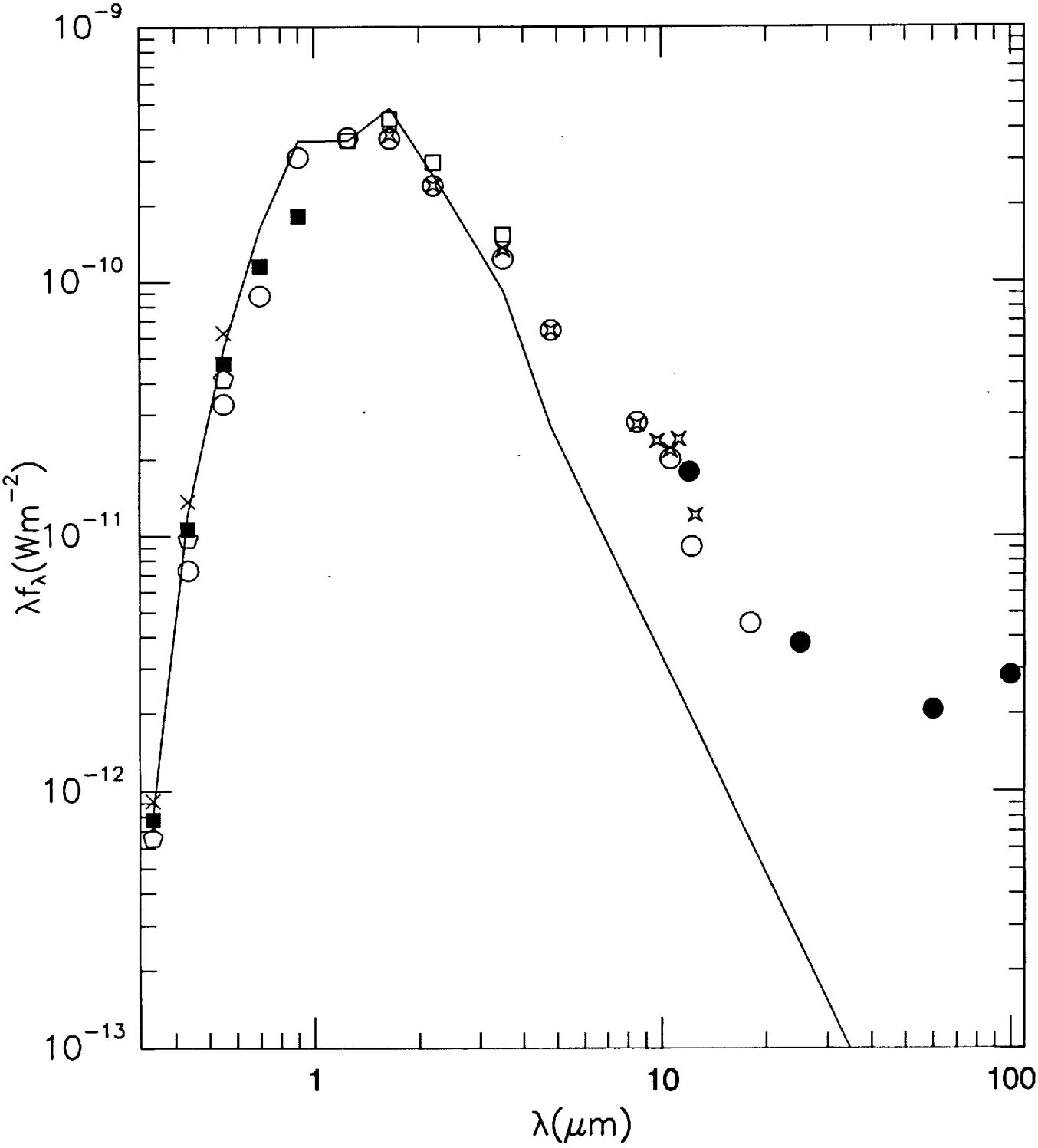
10^{-9}
10^{-10}
10^{-11}
10^{-12}
10^{-13}
$\lambda f_\lambda (Wm^{-2})$
1
10
100
$\lambda(\mu m)$

FIG. 5.

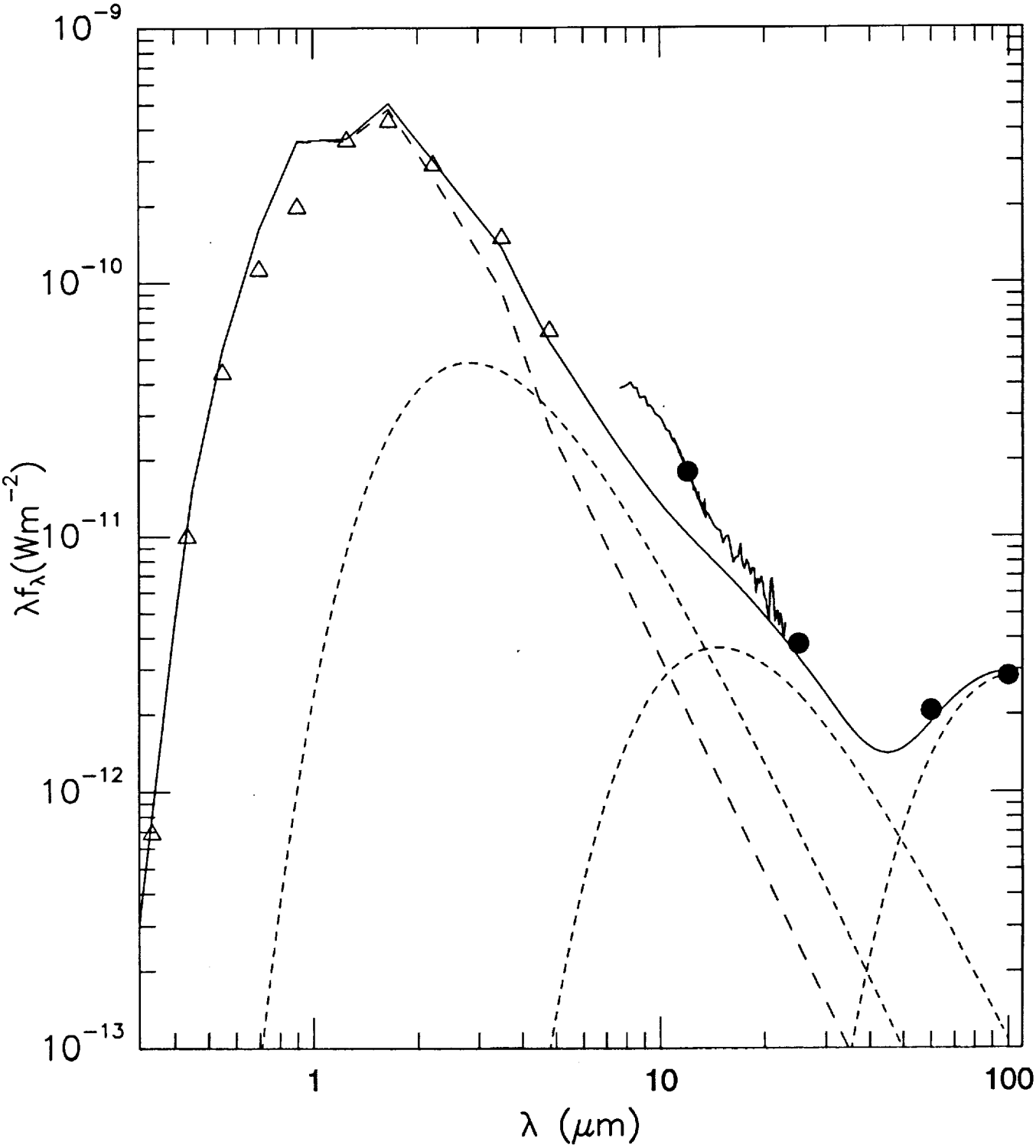
10^{-9}
10^{-10}
10^{-11}
10^{-12}
10^{-13}
$\lambda f_\lambda (Wm^{-2})$
1
10
100
λ (μm)

FIG. 6

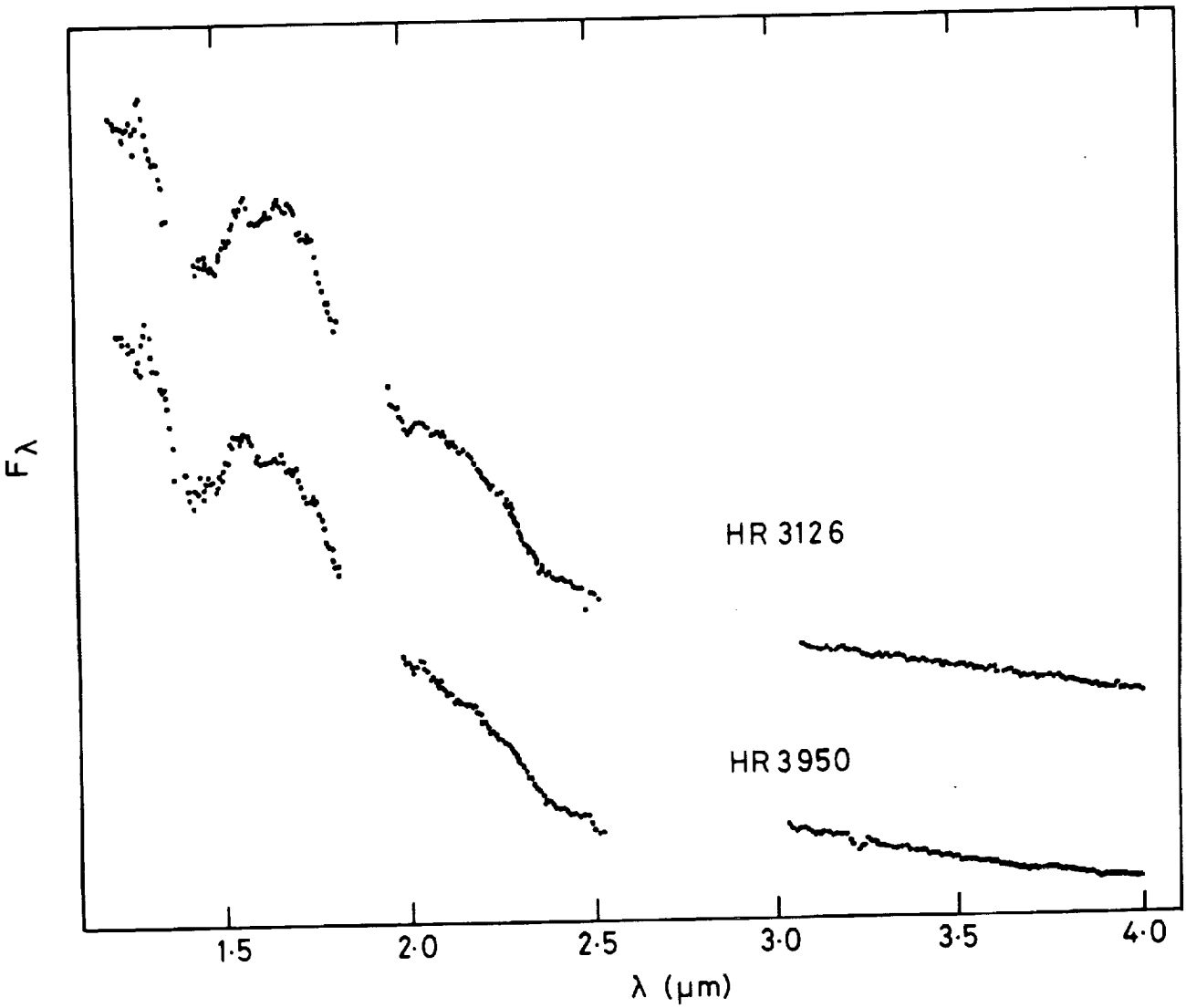

FIG. 7.

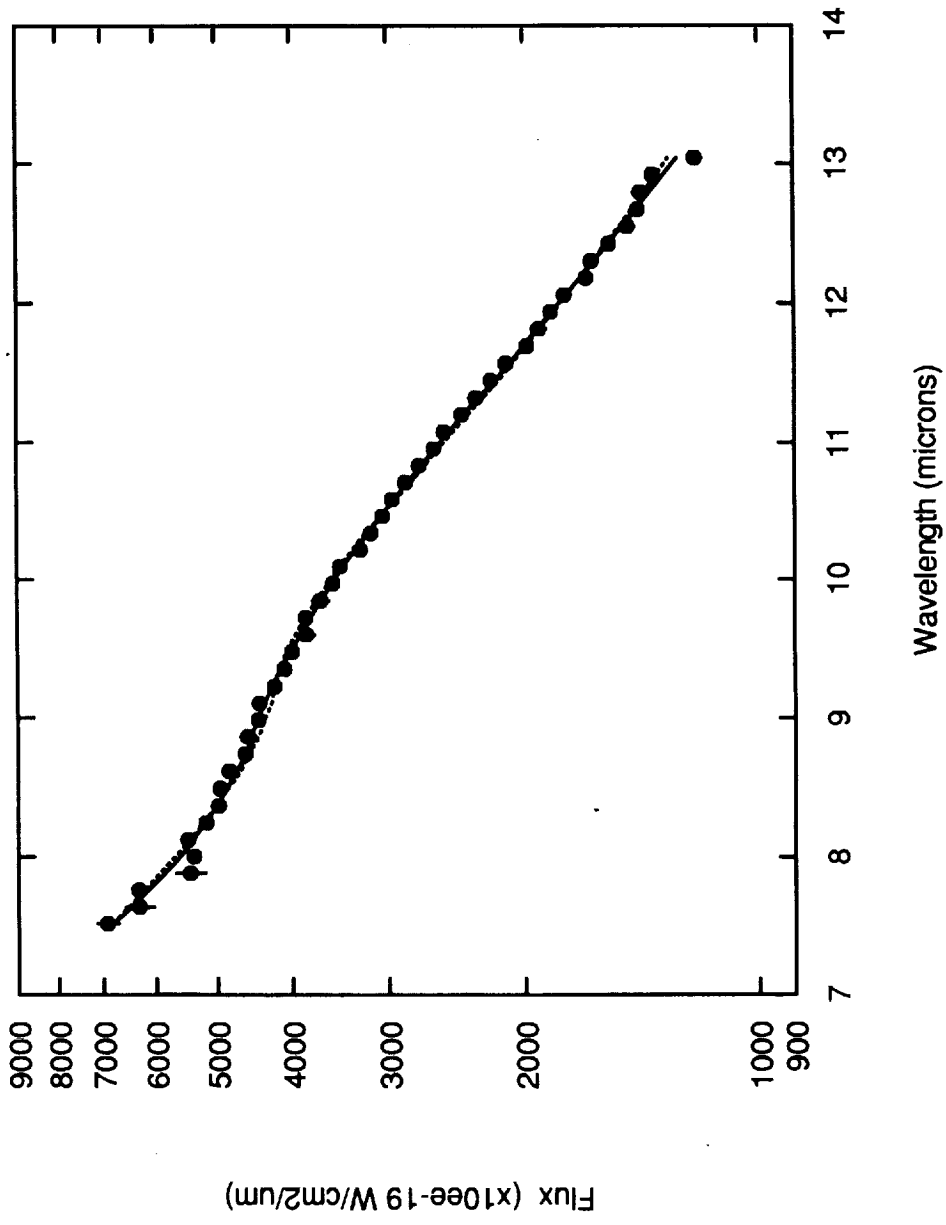
Flux (x10ee-19 W/cm2/um)
9000
8000
7000
6000
5000
4000
3000
2000
1000
900
7
8
9
10
11
12
13
14
Wavelength (microns)